

## Durham E-Theses

---

# *The electrification of newly formed clouds of water droplets*

Najat A. M. Hamdan

### How to cite:

---

Hamdan, Najat A. M. (1971) The electrification of newly formed clouds of water droplets. Masters thesis, Durham University.

### Use policy

---

The full-text may be used and/or reproduced, and given to third parties in any format or medium, without prior permission or charge, for personal research or study, educational, or not-for-profit purposes provided that:

- a full bibliographic reference is made to the original source
- a <https://etheses.durham.ac.uk/id/eprint/10027/> is made to the metadata record in Durham E-Theses
- the full-text is not changed in any way

The full-text must not be sold in any format or medium without the formal permission of the copyright holders.

Please consult the [full Durham E-Theses policy](#) for further details.

THE ELECTRIFICATION OF NEWLY  
FORMED CLOUDS OF WATER DROPLETS

by

MRS. NAJAT A. M. HAMDAN, B.Sc.

Presented in Candidature for the Degree of  
Master of Science in the University of Durham

June 1971

### ABSTRACT

A survey of previous work on cloud droplet electrification was carried out. A cloud chamber was constructed and used to generate droplets of radius in the range 1-3  $\mu\text{m}$ . The size and the charge of individual droplets were determined. Positive and negative droplets were observed. The average charge on the droplets was found to be about  $5e$ . Also a photographic method was tried and discussed to determine the charge on the droplets.

Definition of the Symbols used in Chapter (1) section (3)

Ac	Alto cumulus
As	Alto stratus
Ac cast.	Ac castellanus
Ac lent.	Ac lenticularis
Cb	Cumulonimbus
Cc	Cirrocumulus
Ci	Cirrus
Cs	Cirrostratus
Cu	Cumulus
Cu fr.	Cu fractus
Ns	Nimbostratus
Sc	Stratocumulus
Sc cuf.	Sc cumuliformis
Sc vesp.	Sc Vesperalis
St	Stratus

# C O N T E N T S

## PART I

<u>CHAPTER 1</u>	<u>CLOUDS</u>	<u>Page</u>
1.1	Introduction	1
1.2	Formation of clouds	2
1.3	Classification of clouds	2
1.4	Water content of clouds	9
<u>CHAPTER 2</u>	<u>CLOUD DROPLETS</u>	
2.1	Condensation nuclei	11
2.2	Sizes and numbers of cloud droplets	13
2.3	Theoretical studies of cloud droplet growth	14
2.3.1	Growth of a droplet by condensation	14
2.3.2	Growth by accretion	17
2.3.3	The growth of a population of droplets	19
2.4	The fall velocity of drops	20

## PART II

<u>CHAPTER 3</u>	<u>THE ELECTRIFICATION OF CLOUDS</u>	
3.1	The vertical potential gradient and current in fine weather	22
3.2	Charge generation in clouds	24
3.3	Lightning	26
3.4	Electrical and meteorological conditions inside thunderclouds	27
3.5	The electrical structure of thunderstorms	30
<u>CHAPTER 4</u>	<u>NIMBOSTRATUS CLOUDS</u>	
4.1	Introduction	32
4.2	The electrical structure of nimbostratus clouds	32
4.3	A proposed model for nimbostratus clouds	33
4.3.1	The general case	34
4.4	Relation between precipitation current and potential gradient	36

	<u>Page</u>
CHAPTER 5 <u>A SURVEY OF PREVIOUS WORK ON CLOUD DROPLET ELECTRIFICATION</u>	
5.1 Introduction	39
5.2 Work in the period up to 1946	39
5.3 GUNN 1947-1955	40
5.4 SARTOR 1954	42
5.5 WEBB and GUNN 1954	44
5.6 BLANCHARD 1955	44
5.7 TWOMEY 1956	45
5.8 PHILLIPS and KINZER 1957	46
5.9 ALLEE and PHILLIPS 1958	47
5.10 SHISHKIN 1963	48
5.11 AZAD and LATHAM 1959	48
5.12 LATHAM and SMITH 1969	49
5.13 COLGATE and ROMERO 1970	50
<u>PART III</u>	
CHAPTER 6 <u>A LABORATORY EXPERIMENT</u>	
6.1 The diffusion chamber	51
6.2 Operation of the chamber	52
6.3 Measurement of charges	53
CHAPTER 7 <u>THE OBSERVED CHARGES ON THE DROPLET</u>	
7.1 Results and data analysis	54
7.2 Suggestions for further work	56
ACKNOWLEDGEMENTS	57
REFERENCES	58

# CHAPTER 1

## CLOUDS

### 1.1 Introduction

Water vapour plays a very special role in atmospheric phenomena. Whereas nitrogen, oxygen and the inert gases are present in the atmosphere in constant proportions, the water vapour content is subject to very wide variations. Further, water vapour can pass into the liquid or solid phase and can interact with land and sea surfaces, which evaporate moisture and recover moisture in the form of precipitation. At the temperatures prevailing in the atmosphere, water may exist in all three states. Further, water vapour is capable of saturating space. All this produces a continuous circulation of water in the atmosphere. The water vapour evaporated from the surface of seas and humid land is dispersed in the atmosphere through turbulence and by ascending horizontal air currents.

It was mentioned above that one of the links in the hydrologic cycle is the condensation of vapour and formation of cloud. However, the definition of cloud as the product of vapour condensation needs to be amplified. Strictly speaking, the primary products of condensation are cloud elements, or moisture droplets. These elementary droplets undergo continuous transformation - they form, grow, evaporate, vanish; their size and number vary, they collide, fuse, freeze and crystallize. The concept "cloud" embraces a set of droplets and crystals in a continuous state of evolution. The properties of this set also depend on the velocity of the air which carries it and on the temperature and humidity changes taking place inside it. Temperature variations in a cloud in turn depend on the liberation or absorption of latent heat and on the emission of heat by cloud particles, i.e. on processes that are themselves capable of assisting the development of

vertical motions in a cloud. A cloud is the manifestation of a complex thermodynamics process.

### 1.2 Formation of clouds

Clouds form in the free atmosphere almost entirely as a result of the expansion and consequent cooling of ascending air. The process may be studied in its simplest form by considering the history of a parcel of air which is lifted adiabatically, although matters are often complicated by the fall-out of precipitation, and by mixing between air-parcels of different properties. It follows from the conservation of energy that in such a parcel of cloud-free air, the temperature decreases, as the parcel rises, at nearly  $10 \text{ deg km}^{-1}$ . At the same time, the partial pressure of water-vapour in the air is reduced, in proportion to the total pressure, so that the dew-point of the air also falls although much more slowly than the temperature, about  $2 \text{ deg km}^{-1}$  depending on the temperature and pressure. If the lifting continues far enough the temperature will eventually reach the dew-point and then condensation will begin. From this point on, the situation is more complex, since condensation releases a large amount of latent heat. In tropical air, which is rich in condensable water-vapour, the subsequent rate of cooling, as the saturated or wet adiabatic lapse-rate, is only about one half of the dry adiabatic lapse-rate. In polar regions, or in the upper parts of the troposphere, there is little difference between the two lapse-rates. The prevailing lapse-rate determine the stability of the atmosphere.

### 1.3 The classification of clouds

In the recent years several attempts have been made at creating a genetic classification of clouds based on an analysis of the processes of

formation. BERGERON (1934) suggested dividing clouds into three classes: proper cumuliform, wave and proper stratiform. He advanced this as a morphological classification, although essentially it should have reflected the physical processes of cloud genesis. This idea has retained its value to the present day. Further, BERGERON suggested a genetical-physical classification, for use in conjunction with the preceding one, based on the microstructure of clouds and on the presence of precipitation such as ice needles, snow powder, stable fog, drizzle and rain. KRICHAK (1952) suggested a new genetic classification comprising the following types:-

- 1 - Clouds of regular ascent [Ci, Cs, As, Ns, Ac, Sc];
- 2 - Clouds of nonadiabatic cooling [fog, St, Sc, Ac, As];
- 3 - Clouds of thermal convection [Cu, Cb, Ac, Cast., Cc];
- 4 - Clouds of dynamic convection [Cu, Cb, St, Sc, Cu fr., Cc];
- 5 - Sheet clouds and bumpy clouds (clouds of vertical development) [Ac lent., Sc cuf., Sc vesp., Ac, Cc].

The simplified classification of clouds is the morphological classification. It is a foundation of modern cloud atlases. Its major features are apparently here to stay. It is a good working tool for all synoptic meteorologists and cloud physicists and is used in the International Cloud Atlas (1957). The problem of a morphological classification has a fairly long history. The first classification, given by LUKE HOWARD in (1803), distinguished three main "modification" of clouds - cirrus, cumulus and stratus - and a fourth, complex one, combining the first three and called by him "rain" clouds. Later HILDEBRANDSSON (1887) and ABERCROMBIE suggested a classification composed of ten main forms. This classification closely resembles the one in use today.

The present morphological classification is today of very great value both for practical synoptic work and aviation and for research. It is used

by all meteorological stations the world over, and enables the collection of fast and uniform observational data. At the same time it provides a fairly clear, though incomplete, view of the processes taking place in the atmosphere and of the atmosphere's stability and movement. The same physical processes acting at different altitudes in the atmosphere will give rise to somewhat different cloud forms. The size, density and general form of the clouds will depend on the decrease in specific humidity and on the temperature lapse. For this reason in meteorological observations it is customary to divide clouds into three levels: usually the high level includes clouds lying above an altitude of 6 km, the middle level clouds with a base between 2 and 6 km and the low level clouds with a base below 2km. This division into levels is, however, to a significant extent arbitrary. A given cloud form may occur at very different altitudes. Thus, ordinary cumulus clouds may be formed both near the ground and at altitudes up to 6-6.5 km; cirrus, on the other hand, which is typical of high altitudes, may drop nearly to ground level in cold climates. In mountains the assignment of clouds to given levels is even more arbitrary.

High clouds include the following:

1. Cirrus clouds [Ci]: These are white, wispy clouds, generally very thin and transparent, sometimes thickening in places in irregular masses or tufts. Usually they are so transparent that the sky shows through them, and the sun or moon shine so brightly that objects throw shadows. Cirrus clouds may consist of individual strands [Ci filorus], sometimes very tangled [Ci intortus] and sometimes with thickened ends bending upward [clawlike, Ci uncinus]. The latter may indicate the bands of Ci are extending from small denser clouds arranged in rows, or, on the contrary, that small denser masses form above places where condensation is taking place and snowflakes are falling. Occasionally the dense masses of cirrus

represent the residue of anvil clouds, either retaining this shape [Ci incus - genitus] or dispersed [dense cirrus, Ci spissatus].

2. Cirrocumulus clouds [Cc]: are thin semi-transparent cirrus clouds occasionally assume the shape of ripples, scales or regular rows of very fine undulating cloud flakes, and are then called Cc. Frequently one section of a Ci layer may have an undulating structure while another section does not. Certain Cc clouds may be shaped like irregularly dispersed shreds [Cc flocus]. Sometimes the entire mass of Cc cloud assumes the shape of large lenses extending across the sky [Cc lenticularis].

Cirrocumulus actually also includes the condensation trails that are often formed in the upper layers of the atmosphere 7-13 km behind upper layers.

3. Cirrostratus clouds [Cs]: are thin and fairly uniform white or bluish cloud film which may produce a somewhat undulating pattern [thread-like, Cs filusus] or may form a uniform veil [foglike, Cs nebulosus]. Cirrostratus clouds may display marked optical phenomena: halo around the sun, radius 22 to 46°, horizontal circle passing through the sun, false sun and moon and other less frequent phenomena.

Cirrus cloud forms still remain the least studied in aerology. Since the upper troposphere probably has a fairly wide variety of physical processes of cloud formation such as, convection, turbulence, wave motion, a careful study of cloud forms would be of great value.

The middle clouds usually from 2 to 6 km comprise altostratus and altocumulus clouds.

1. Altostratus clouds [As]: are grayish or slightly bluish film, sometimes slightly fibrous or wavelike, covering the entire sky. They may be so translucent that the sun and moon shine through as light spots

[translucent, As translucidus]. In other cases they may be fairly dense [opaque, As opacus] and the celestial bodies are hidden. Both form may be precipitating, for example with snow reaching the ground in winter. Brightly coloured coronas around sun and moon may be seen in thin As.

2. Altcumulus clouds [Ac]: These are light-coloured ripples, rolls, small puffs or flakes between which the blue sky is nearly always seen. Occasionally they fuse in a continuous mantle, comparatively thin [opaque, Ac opacus], as distinct from the translucent variety [Ac translucidus]. Fairly often they are shaped like lenses or cigars with a smooth outline [Ac lenticularis]. Certain subclasses of Ac bear the mark of the convection that takes place inside them. Such are the Ac castellatus, similar to small Cb storm clouds, or Ac floccus, similar to small dissolving Cu cong. Ac may produce precipitation which is seen as band or tails reaching the ground [Ac virga]. Ac clouds form a comparatively thin layer and the sun may shine through its edges. Bright rainbow colours are often seen on the thin margins of Ac.

Low clouds include the following:

1. Stratocumulus clouds [Sc]: are very similar to altcumulus although lying at a much lower level, usually at altitudes of up to 2 km. They are shaped like large waves or ridges or even large plates. In the gaps between them the cloud cover is thinner and the sun or moon may shine through [Sc translucidus], but blue sky is rarely seen. More frequent are the opaque stratocumulus [Sc opacus]. A class of cumuliform stratocumulus [Sc cumuliformis] associated with processes of ordinary convection in the atmosphere may be distinguished. Of these the Sc castellatus connote a process similar to the formation of downpour clouds. The daytime [Sc diurnalis] and evening [Sc vespertalis] stratocumulus clouds are the

product of the dissolution of cumulus clouds, either under an inversion or in the evening when cumulus clouds settle and disperse. The Sc, as well as Ac and Cc, clouds are the results of a combination of undulatory motions and the appearance of the so-called cellular circulation of the atmosphere.

2. Stratus clouds [St]: Form a low grey film, sometimes nearly uniform and sometimes very tattered in the lowermost part with irregular pieces hanging down. Seen from below their shape reflects the turbulent process which gave rise to them and irregular air motions of different sizes. In addition to the ordinary fog-like stratus clouds [St nebulosus], certain St clouds sometimes show an undulating pattern [St undulatus]. Stratus clouds are usually opaque, though all stages of St, from scattered fragments [St fractus] to a dense layer may be observed. A special and very interesting subclass is the fractonimbus, which form a tattered cover under clouds with heavy or prolonged precipitation [Ns,As,Cb].

The third form of low cloud, Ns, are similar in external appearance to stratus clouds.

3. Nimbostratus clouds [Ns]: are solid grey, or yellow-grey veil, nonuniform and in places even seemingly translucent. They are generally much thicker than St, though an observer looking at them from below would not always be able to evaluate their thickness. Ns clouds give prolonged precipitation and are nearly always associated with fronts. The large zones of Ns-As are therefore easily distinguishable from St zones on synoptic maps. In their interior Ns clouds are high nonuniform and include fairly large light patches and even cloudless horizontal layers. Under Ns clouds are frequently seen the tattered fractonimbus clouds. Ns masses sometimes contain isolated Cb clouds. Such clouds produce torrential heavy and short lived rain. On the edges of cyclones, nascent and dying Ns clouds are thin

1-2 km and nonprecipitating.

Clouds of vertical development comprise the following:

1. Cumulus clouds [Cu]: these are separate dense white clouds consisting of puffs or caps with a flat and darker base. They are always separated by gaps. There are various transitional stages, from nascent [Cu fractus], low [Cu humilis], middle [Cu mediocris] to thick [Cu congestus] cumulus, whose summit occasionally reaches 6-7 km. The shape of these clouds makes it possible to recognise the presence of ascending flows, large-scale turbulence and variation in wind velocity at different altitudes, due to which the cloud tops may be bent in one direction.

2. Cumulonimbus clouds [Cb]: these are seen in last stage of development of cumulus, sometimes reaching altitudes of 20.5 km in tropical zones. They are characterized by scattering of the topmost layer of a cloud which loses its puffy shape and changes into a horizontal mass of cirrus cloud. Bald cumulonimbus clouds [Cb calvus] which are scattering but have not yet assumed a fibrous cap should not be confused with the "hairy" cumulonimbus [Cb capillatus] which have. The latter often assume the shape of an anvil [Cb incus]. The cumulonimbus are sometimes referred to as a "cloud factory" because, aside from cirrus cloud, upon dissolving into lower levels they give rise to layers of altostratus, typical of tropical zones, and altocumulus. They are often accompanied by lenslike clouds, various classes of stratocumulus, and so on.

There are several cloud groups which do not fit into the morphological scheme including for example, Mother-of-pearl clouds and Noctilucent clouds.

#### Mother-of-pearl clouds

Mother-of-pearl clouds show their iridescent colours more clearly than ordinary wave clouds when they are illuminated by the setting sun after it

has ceased to shine on the troposphere. The surrounding sky is dark and the sun itself does not dazzle the observer. They may occur most commonly in north-westerly air currents which extend up to 20 km or more. Parts of them show the bright iridescent colours which give them their name. These parts have well-defined edges. They are accompanied usually by diffuse veils or trails which appear to stream from the lee edges of the coloured, sharply defined, clouds. They are observed to be at heights between 18 and 30 km, most commonly somewhat above 20 km. Such temperature measurements as are available in the neighbourhood suggest that they exist at about  $-80^{\circ}\text{C}$ , which is several degrees lower than the seasonal average for their altitude and geographical position.

#### Noctilucent clouds

Observations of these clouds provide information concerning the physical state of the upper atmosphere at the height of about 80 km at which they invariably occur. Besides yielding direct measurements of wind, they indicate the existence of a temperature minimum at 80 km. Since they are made visible by the sunlight scattered by the material of which they are composed, they are observed only on nights when the sun remains close below the horizon, that is, during the summer months in middle latitudes. Presumably they may be present at other times and in other latitudes, but they will not remain sunlit long enough to be observed. Their nature is still in doubt, though their tendency to appear at times of comet and meteor occurrences strongly supports the belief that they consist of meteoric dust.

#### 1.4 Water Content of Clouds

The water content i.e. mass of water in the liquid or solid phase per unit volume of air, is of considerable meteorological importance. Its

magnitude and spatial distribution indicate the degree of mixing which has taken place between the rising cloudy air and its drier environment. Changes in the water content are important thermodynamically, since they are accompanied by large energy changes. The first attempt at measuring the water content was made by SCHLAGINTWEIT in (1851) in mountains in dense fog. Three observations yielded water contents of  $3.83 \times 10^3$ ,  $3 \times 10^3$ ,  $1.53 \times 10^3$   $\text{kgm}^{-3}$ . These measurements remained unique until the end of the nineteenth century, when CONRAD (1899) and WAGNER (1908) carried out a limited number of measurements of the water content of clouds. The absence of systematic measurements of water in clouds was due to the lack of equipment for aerial ascents and of a simple and reliable method of measurement. The practical significance of this element remained unclear for a long time.

It was only after (1945) that data on cloud water content became necessary in connection with research on aircraft icing, design of anti-icing devices, development of methods for influencing clouds and inducing precipitation, analysis of conditions of absorption of ultra-short waves. It can definitely be assumed that in mixed clouds where the solid ice water content is low compared with the liquid-water content. It should also be remarked that where precipitation is taking place from the clouds, one is actually measuring the water content not only of the cloud proper, but also of the precipitation, which is particularly significant in the lower cloud layer. It can be assumed from the start that the cloud water content depends on the temperature and temperature gradient of the cloud, height above the base, phase and form of the clouds and, finally, thermodynamic conditions of cloud development. In space the water content fluctuates considerably, frequently increasing or decreasing several times over a distance of some hundreds of metres. Sometimes in stratocumulus clouds the variation in water content is subject to a fairly pronounced periodicity, while in other instances, as in cumulus clouds, the sharp changes display no regularity.

## CHAPTER 2

### CLOUD DROPLETS

#### 2.1 Condensation nuclei .

In the perpetual interactions between the surface of our planet and the lower atmosphere there is a continuous exchange of gaseous components and of liquid and solid particulates as well. Locally these processes are strongly augmented by man's activities. From the outer atmosphere another class of particulates mainly thought of as meteoritic dust, is contributed. Depending on their physical and chemical nature, particles are suspended for a period of time varying between minutes and years. Gravitational fall-out ceases to be significant for particles of diameter less than about  $3 \mu\text{m}$ . At this size begins the range of the aerosols. They might remain airborne indefinitely were it not for their occasional encounter with clouds and precipitating water which washes some of them out of the atmosphere. While the upper limit of size of aerosols is determined by gravitational removal, the lower limit is not clearly defined. The definition involves the border-line between a molecule in the free, gaseous state and an embryo particle.

The most common limitation of size at the lower end of the scale comes about through coagulation. In this process the smallest, most mobile members collide and stick together to form larger, less mobile and thus more stable particles. The various processes in the lower atmosphere have the net effect of producing a range of roughly  $0.01$  to  $1 \mu\text{m}$  in concentrations between  $10^8$  and  $10^{10} \text{ m}^{-3}$ . From measurements at the ground, JUNGE (1958) has equated the product of the size and number density of aerosols to their total volume in each size class and has found that the volume of aerosol per given volume of air is about the same in all size classes from about the same in all size classes from about  $0.1$  to  $10 \mu\text{m}$  radius.

Ions form a special class of aerosol. They are continuously being created in the atmosphere by cosmic radiation and over the continents from the radioactive gases emanating from the soil. Under favourable conditions there may be  $10^8$  to  $10^9$  small ions  $m^{-3}$  near sea level, increasing with height to about  $10^{11}$  or more  $m^{-3}$  in the ionosphere. There is an inverse relation between the number of small ions and the number of large aerosols at any one time and place. The common aerosols capture the ions and so make their mobility very small. In fact, it is found that the more numerous aerosols provide an effective means of reducing the number of small ions, by this capture process. About half of the aerosols in the 0.01 to 0.1  $\mu m$  range carry a net charge as a result of ion capture and therefore are classed as large ions. They have mobilities of less than  $10^{-7} m^2 V^{-1} s^{-1}$  contrasted with the mobilities of about  $10^{-4} m^2 V^{-1} s^{-1}$  for the small ions.

Small ions become important for condensation only when the air is cleaned of other aerosols. The large supersaturations required before they can serve as centres of condensation make them ineffective in the natural atmosphere. High water vapour content and near-micron-sized aerosols usually are found together because they both come from the same source - the surface of the earth. It is convenient to divide the spectrum of potential condensation nuclei into three parts: (a) those nuclei which can be detected in an Aitken counter, having radii between  $5 \times 10^{-3} \mu m$  and  $0.2 \mu m$ , and which are called 'Aitken nuclei'; (b) particles of radii between  $0.2 \mu m$  and  $1 \mu m$ , which are called 'Large nuclei'; and (c) particles larger than  $1 \mu m$  radius which may be called 'Giant nuclei'. Division according to these particular size groups has the advantage that it coincides quite well with divisions based either on the techniques used for measuring the particles, or on the processes by which they are produced. The relative concentrations of the three classes of nuclei as determined by JUNGE at Frankfurt are shown in

table 2.1, where the values are the mean of 25 sets of measurements.

TABLE 2.1

Relative concentrations of Aitken, large and giant nuclei.

	Aitken	Large	Giant (drops and solid particles)			
			r = 1-2	2-3	3-5	5-10 $\mu\text{m}$
Mean concentration $\text{m}^{-3}$	$4.25 \times 10^{10}$	$1.32 \times 10^8$	$8.03 \times 10^6$	$8.8 \times 10^4$	$2.44 \times 10^4$	$5.1 \times 10^3$
Mass ( $\mu\text{g m}^{-3}$ )	17	26	23	4.2	5.1	9.1

## 2.2 Sizes and numbers of cloud droplets

The spectrum of cloud-droplets sizes varies from one cloud type to the next, from one cloud of one type to another cloud of the same type. As a matter of fact, from one place and time to another place and time in the same cloud, there are large differences in the droplet characteristics. But even with all these variations, on average, the droplets in certain types of clouds are considerably different from those in other clouds. Fig.2.1 shows how the numbers of droplets of various sizes differ in three types of cloud in the cumulus family. Cumuli of fair weather seldom are more than 0.9 km, and often are less than 0.3 km, thick. They never produce rain. It can be seen that in these clouds the droplets are small and numerous. The maximum diameters in most of them are less than  $50 \mu\text{m}$  and the concentrations of droplets are above  $3 \times 10^8 \text{ m}^{-3}$ .

In large cumulus clouds, which produce showers, it is found that the droplet diameters often exceed  $50 \mu\text{m}$ . The concentrations of droplets are

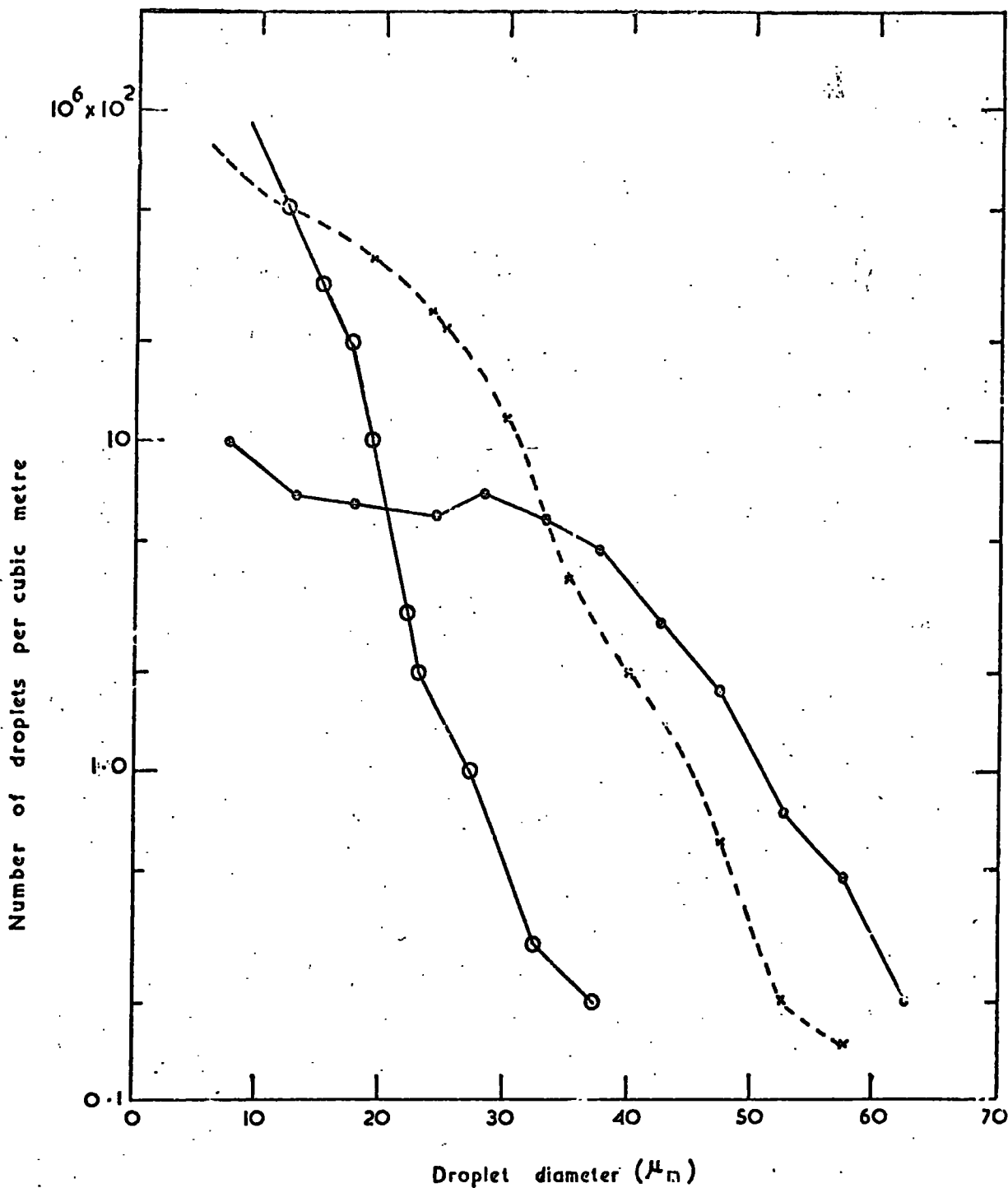


Fig.2.1 The spectrum of droplet sizes in three types of clouds.

--x--x-- Large cumulus over the central United States, total number of droplets =  $22 \times 10^7 \text{ m}^{-3}$ .

—o—o— Cumulus of fair weather, total number of droplets =  $3 \times 10^8 \text{ m}^{-3}$ .

—:— Cumulus over tropical ocean, total number of droplets =  $55 \times 10^6 \text{ m}^{-3}$ .

smaller than in fair-weather cumuli, they are about  $2 \times 10^8 \text{ m}^{-3}$ . The cumulus clouds over tropical oceans have droplet characteristics differing markedly from those found in continental clouds. Cumulus clouds over continents seldom produce rain unless their summits rise as high as 4 to 7 km. The droplets in tropical clouds occur in concentrations of only about  $6 \times 10^7 \text{ m}^{-3}$  but there are usually some droplets of diameters exceeding 50  $\mu\text{m}$ . It has been suggested that the presence of many large cloud droplets in shallow clouds can be attributed to a large number of giant salt nuclei.

In layer-type clouds the droplets are usually smaller than in cumuli-form clouds. Measurements by a number of investigators have shown that in most stratified clouds the average droplet radii range in size from about 4 to 10  $\mu\text{m}$  while the concentrations range from about  $2 \times 10^8$  to  $6 \times 10^8 \text{ m}^{-3}$ . In shower clouds the average radii are near 20  $\mu\text{m}$ , and concentrations are  $5 \times 10^7$  to  $2 \times 10^8 \text{ m}^{-3}$ .

### 2.3 Theoretical studies of cloud droplet growth

There are two conceivable processes by which nucleus droplets may attain radii of several microns and so form a cloud or fog; the diffusion of water vapour to and its condensation upon their surfaces, and growth by the coalescence of droplets moving relative to each other by virtue of Brownian motion, small-scale turbulence, and differential rates of fall under gravity.

#### 2.3.1 Growth of a droplet by condensation

Saturation occurs when moist air has such a composition that it can exist in equilibrium with a plane surface of pure water at the same temperature as the air. Here the term equilibrium means that there is no net transfer of water vapour molecules from the air to the water surface or from

the water surface to the air. This equilibrium then defines the saturation vapour pressure and 100 per cent relative humidity. The equalifications that the water must be pure and that the surface must be plane are important, for if the water is not pure or if the surface is not plane, other equilibria will exist, for example, that ordinary NaCl salt gets wet long before the relative humidity reaches 100 per cent. Therefore, if the droplet contains salt it can be in equilibrium with the surrounding air when the relative humidity is less than 100 per cent. The difference depends upon the strength of the solution, and this is expressed as the solute effect.

If a salt nucleus is introduced in moist air which is not saturated, condensation will then occur on the salt. However, as the droplet grows the solution weakens, and the growth of the droplet will be more or less as shown by curve A in Fig.2.2. When the drop has grown so that its radius is about 2  $\mu\text{m}$  it is so diluted that, for all practical purposes, it behaves as if it were pure water. Thus, the solute effect is important only at the very beginning of the process, but during this phase it is all important, since droplets would not form if nuclei were absent.

The solute effect is counteracted by another called the curvature effect. When the drops are very small the surface tension is important. The "skin" of a droplet, like that of a soap bubble, behaves like a stretched membrane, and work must be done to stretch it further. In fact, this means that such a droplet will resist the advances of the vapour molecules in the air until the vapour pressure is greater than the saturation value corresponding to a plane water surface. In other words, a small droplet will not be in equilibrium with the surrounding air until the relative humidity is over 100 per cent. If a small droplet of pure water is introduced into supersaturated air with such high humidity, the drop begins to grow. The curvature of the droplet then decreases, and as the growth

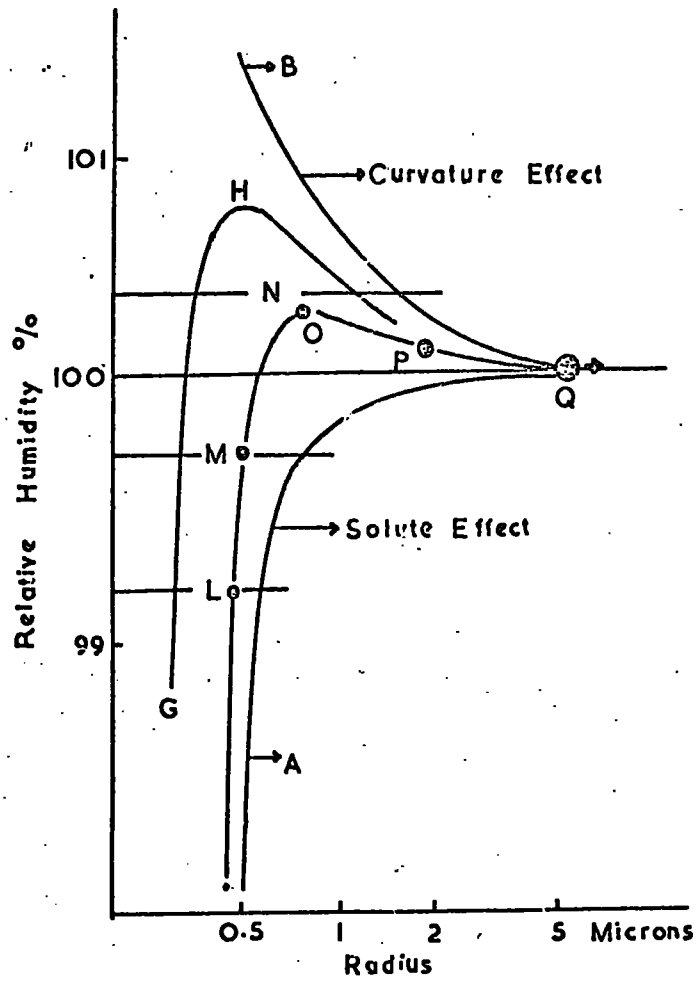


Fig.2.2 Showing the formation and growth of cloud droplets.

progresses the effect of curvature tends to vanish, more or less as shown by curve B in Fig.2.2. When the droplet has grown so that its radius is 2 to 3  $\mu\text{m}$ , the curvature effect is so small that, for all practical purposes, the drop behaves as if it had a plane surface. It will thus be seen that both the solute effect and the curvature effect are important only at the very beginning; later the process is almost the same if the water were pure and the surface plane.

The actual growth comes out as a compromise between the solute effect and the curvature effect, as shown in Fig.2.2. Suppose that a nucleus of salt is introduced into air which is not saturated. The nucleus will then absorb water until it is in equilibrium with the surrounding air. This point be indicated by L in Fig.2.2. Next let the air be cooled so that the relative humidity increases a little. The droplet will grow further until a new equilibrium is reached at M. The air is now cooled again so that the relative humidity increases to the value indicated by N. The droplet will then grow along the curve LMOP without coming into equilibrium with the surrounding air. After the hump O has been passed, the growth is unstable in the sense that it does not result in an approach to equilibrium. If a much smaller nucleus were used, the solute effect would be smaller and the curvature effect larger. The result would be that the hump H would be higher, as indicated by the curve GH.

Computations show that it takes an average nucleus about 1 s to grow to 10  $\mu\text{m}$ , a few minutes to grow to 100  $\mu\text{m}$ , 3 hrs to grow to 1,000  $\mu\text{m}$  or 1 mm, and about a day to grow to 3 mm. Since heavy rain may develop within an hour or two after the cloud has formed, it is evident that the condensation process is far too slow to account for the formation of raindrops, although it is able to produce drops of drizzle size.

### 2.3.2 Growth by accretion

#### (a) Equation of growth

A drop which is larger than, and consequently acquires a velocity relative to its smaller neighbours, will overtake and collide with some of those lying in its path. It is shown by MASON (1955) that if a fraction  $E_2$  of the droplet which collide with the larger drop coalesce with it Fig.2.3, the latter would grow at a rate given by the equation

$$\frac{dm}{dt} = 4\pi R^2\rho \frac{dR}{dt} = E_1E_2\pi R^2W (V-v) \quad (2.1)$$

where  $E_1$  is the collision efficiency,  $E_2$  is the coalescence efficiency,  $W$  the concentration of liquid water in the form of the smaller droplets, and  $V, v$  are the falling velocities of the larger and smaller droplets respectively. The product  $E_1E_2$  will be termed the collection efficiency and denoted by the symbol  $E$ , and  $m, r, \rho$  are respectively the mass, radius, and density of the droplet, and  $R$  the radius of the large drop.

Integration of equation (2.1) shows that a droplet of radius 25  $\mu\text{m}$  falling through air at  $0^\circ\text{C}$  and 900 mb pressure and containing 1g of liquid water  $\text{m}^{-3}$  composed of droplets with  $r = 6 \mu\text{m}$ , would grow to a radius of 30  $\mu\text{m}$  in 12 min., and to 25  $\mu\text{m}$  in 38 min., if the coalescence efficiency  $E_2$  is assumed to be unity. These times are very short compared with those for growth by condensation. The contribution which coalescence may make to the earlier growth of 25  $\mu\text{m}$  droplet is difficult to estimate, because for  $r/R$  ratios greater than 0.2, mutual interference between the flow patterns set up by the larger and smaller droplet will almost certainly become important and invalidate the calculations of collision efficiency.

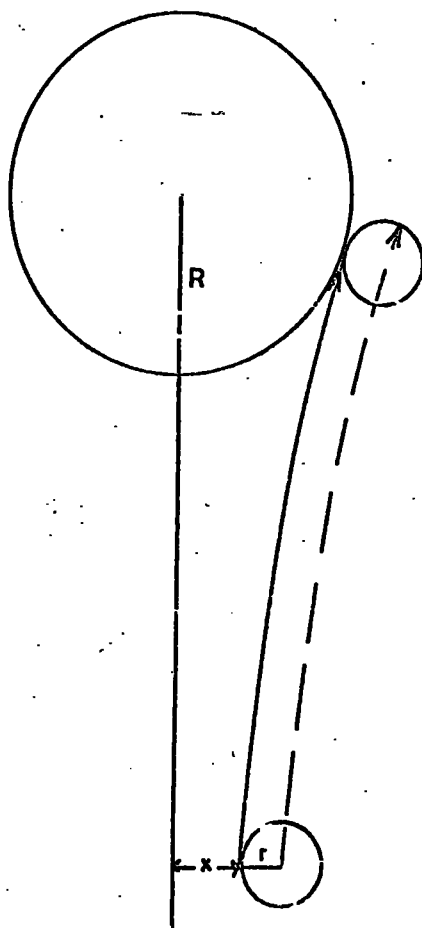


Fig.2.3 Diagrammatic representation of the trajectory of a small drop relative to a large one.

(b) The effect of small scale turbulence on collisions between droplets

It is interesting to inquire whether the number of collisions between cloud droplets of different size might be increased in a turbulent air stream, because if velocity fluctuations of the right frequency occur, the relative velocities between the large and small droplets may be increased owing to differences in their inertia. Clearly there will be an optimum frequency at which the induced relative velocity will be a maximum. At very low frequencies, all the droplets will tend to move with the air, and their relative velocities will be very small; as the frequency increases, the larger drops will lag more and more behind the air motion relative to the smaller ones, but when the velocity fluctuations of the air become short in period compared with the time constant of the smaller droplets, these too will lag, and the relative velocities of large and small droplets will again be small. A theoretical examination of this problem has been made by EAST and MARSHALL (1954). For droplets of radii 15 and 10  $\mu\text{m}$ , the optimum frequency is about 100 cycle  $\text{s}^{-1}$ . If the collision efficiency of larger droplets for smaller ones is to be increased appreciably by the action of turbulence, accelerations of the order experienced when falling under gravity must be imparted to the droplets. This would imply that the air must undergo total root mean square accelerations of the order of  $g$  in the frequency band below about 100 cycle  $\text{s}^{-1}$ . It appears unlikely that turbulence of this intensity occurs in this frequency range in the free atmosphere, and it is accordingly doubtful whether turbulence plays an important role in bringing about collisions between cloud droplets. But EAST and MARSHALL considered only the effect of turbulence on the motion of two drops relative to the air. The effect of spatial variations of the turbulent motion which might lead to collisions, even between droplets of equal size, due to the 'motion of

drops with the air' has been investigated by SAFFMAN and TURNER (1956).

(c) Coalescences between charged and uncharged droplets

The effect of an electrically charged drop on the trajectory of a smaller droplet moving towards it, and hence the effect on the collision efficiency, has been calculated by PAUTHENIER and LOUFTOULLAH (1950). They have calculated the critical distance  $x$  Fig.2.4 within which a small uncharged droplet of radius  $r$  must approach a larger charged drop of radius  $R$ , if collision is to occur by electrostatic forces only. For distance of approach greater than  $x$ , the small droplet is deflected towards the larger drop, but does not collide with it. The collision efficiency  $E_1$  defined as  $x^2/R^2$ , is then given by the expression

$$E_1 = \frac{1}{R^2} \left[ \frac{45}{16\rho g} \frac{\epsilon-1}{\epsilon+1} \frac{q^2}{R^2} \frac{1}{r^2} - 1 \right]^{2/5} \quad (2.2)$$

where  $\rho$ ,  $\epsilon$  are respectively the density and dielectric constant of the water and  $q$  is the charge on the drop. The average charges on large cloud droplets in swelling cumulus are about  $2 \times 10^{-8}$  e.s.u. GUNN (1952); if we substitute this value equation (2.2) and put  $R = 10 \mu\text{m}$ ,  $r = 5 \mu\text{m}$ , the value of  $E_1$  turns out to be 0.043. As larger values of  $R$  will lead to even smaller values of  $E_1$ , it appears that the charges normally present on cloud droplets cannot be of much help in bringing about collisions.

2.3.3 The growth of a population of droplets

In the case of a large population of droplets growing in a rising current of air to form a cloud, there will clearly be some interaction between the growing droplets. LANGMUIR (1944) has shown that with droplets at rest with respect to the air, the separation of droplets in normal clouds

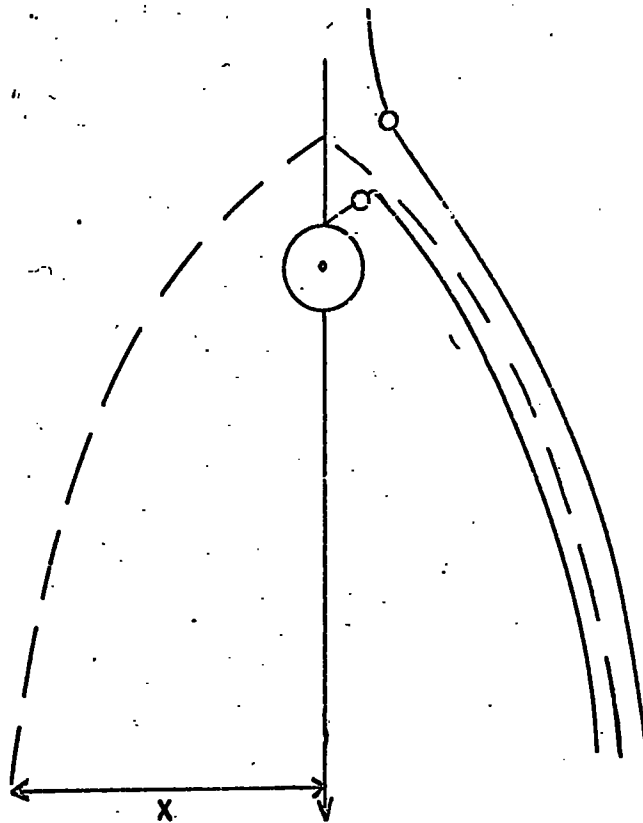


Fig.2.4 The trajectory of a small uncharged droplet relative to a larger electrically charged drop as determined by electrostatic forces. (After MASON).

is so great compared with their diameters that any individual interactions between droplets is negligible. When droplet motion is considered this conclusion is also true, since a typical growing cloud may contain drops of about  $7 \mu\text{m}$  radius, separated from each other by about  $1000 \mu\text{m}$  on the average, and falling relative to the air at about  $5000 \mu\text{m s}^{-1}$ . Every growing droplet therefore experiences essentially the same environment, and the droplets influence each other only through their combined influence on this common environment.

The general outline of the condensation process is a steadily rising current of air is straight forward. As the air rises it expands approximately adiabatically and the saturation ratio increases. Once the saturation point has been passed, condensation begins to occur on the suspended nuclei, the most efficient being activated first. The supersaturation continues to rise more and more nuclei are activated and begin to grow to droplets; the rate increase of supersaturation is, however, now rather lower because the growing droplets are removing the excess vapour from the air. Since large droplets remove water vapour more quickly than do the small ones the excess vapour is soon being removed from the air as quickly as it is being made available by expansion, and thereafter the supersaturation falls towards zero.

#### 2.4 The fall velocity of drops

A water drop will be accelerated downward by gravity. As the velocity increases, the frictional drag against the surrounding air increases, and after a short while the two forces balance. Thereafter the drop falls at terminal velocity. Some typical values for spherical drops are given in Table (2.2). If the air itself had vertical motion, the drops would fall relative to the air with the speeds indicated. It will be seen that a large raindrop can be kept aloft if the updraught is about  $9 \text{ m s}^{-1}$ , and that the

smaller drops would be carried upward in the cloud. Updraughts with such speeds are commonly observed in thunderstorms. When drops of various sizes are present, their rates of fall will vary over wide ranges, and this provides plenty of opportunity for collisions.

When a drop grows to 7 mm in diameter, the fall velocity will be somewhat larger than  $1.06 \times 10^{-2} \text{ km s}^{-1}$ . At such high speeds the drop flattens out and breaks up into a few smaller drops, such as small raindrops and drizzle. Thus there is an upper limit to the size of the drops that can exist in the atmosphere.

TABLE 2.2

Diameter $\mu\text{m}$	Rate of fall	Type of drop
5,000	$8.9 \text{ ms}^{-1}$	Large raindrop
1,000	$4.0 \text{ ms}^{-1}$	Small raindrop
500	$2.8 \text{ ms}^{-1}$	Fine rain or large drizzle
200	$1.5 \text{ ms}^{-1}$	Drizzle
100	$300 \text{ mms}^{-1}$	Large cloud droplet
50	$76 \text{ mms}^{-1}$	Ordinary cloud droplet
10	$3 \text{ mms}^{-1}$	
2	$120 \mu\text{ms}^{-1}$	Incipient droplets
1	$40 \mu\text{ms}^{-1}$	and nuclei

C H A P T E R 3

THE ELECTRIFICATION OF CLOUDS

3.1. The vertical potential gradient and current in fine weather

The fundamental electrical phenomenon on the lower atmosphere is the vertical electric field which, in clear-sky conditions, is directed downwards. This implies that the Earth's surface carries a negative bound charge and the atmosphere a net positive charge. The surface density of charge on the conducting Earth is about  $-3 \text{ e.s.u. m}^{-2}$ , the total fine weather charge amounting to about  $5 \times 10^5 \text{ C}$ . The intensity of the vertical electric field has a maximum value at the ground where its magnitude is the  $120 \text{ V m}^{-1}$  when averaged over the whole earth, and  $130 \text{ V m}^{-1}$  over the oceans; in industrial regions, where the air is highly polluted, the field strength may be considerably enhanced. The surface-field strength  $F_0$  is related to the surface density of charge  $\sigma$  by the equation

$$F_0 = \left( \frac{\partial V}{\partial z} \right)_{z=0} = - \frac{\sigma}{\epsilon_0} \quad (3.1)$$

and has the same sign and order of magnitude in fine weather, over the whole earth. The field intensity or potential gradient decreases at greater heights as shown in Fig.3.1. Thus, the lower atmosphere normally contains a positive space charge of density  $\rho$ , such that

$$\frac{\partial^2 V}{\partial z^2} = - \frac{\rho}{\epsilon_0}$$

where  $V$  is the potential difference between the earth and the atmosphere at height  $z$ . On integration the above equation becomes

$$\frac{\partial V}{\partial z} = \left( \frac{\partial V}{\partial z} \right)_{z=0} = - \frac{1}{\epsilon_0} \int_0^z \rho \, dz \quad (3.2)$$

and the surface value of the potential gradient is given by

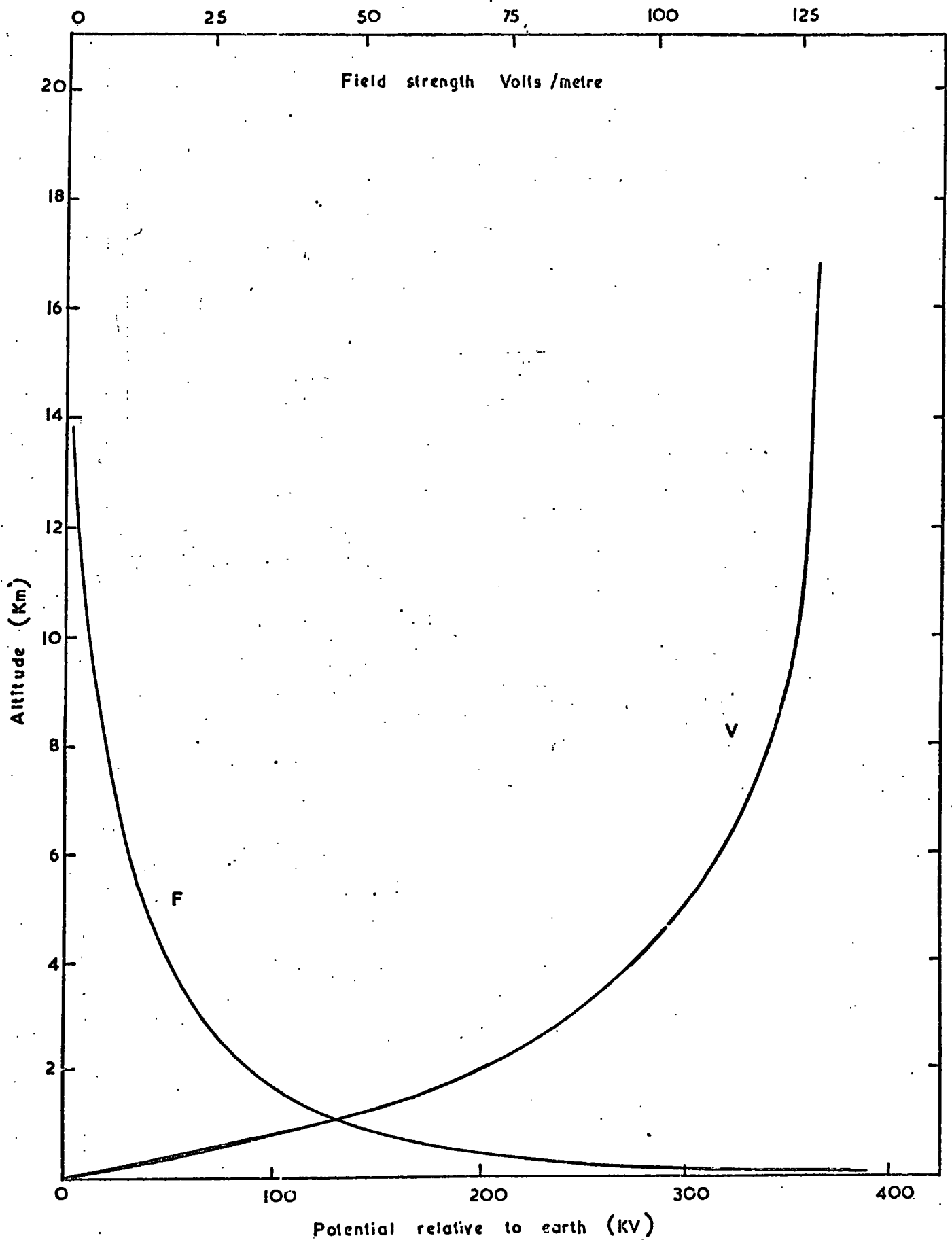


Fig.3.1 The potential  $V$  of the atmosphere and the vertical field strength  $F$  as a function of height. (After MASON).

$$\left(\frac{\partial V}{\partial z}\right)_{z=0} = \frac{1}{\epsilon_0} \int_0^{\infty} \rho \, dz = -\frac{1}{\epsilon_0} \sigma .$$

Thus 
$$\sigma = - \int_0^{\infty} \rho \, dz \quad (3.3)$$

The potential  $V$  of the atmosphere with respect to the Earth surface increases with altitude up to about 20 km, above which it remains sensibly constant at about  $4 \times 10^5$  V, as shown in Fig.3.1. The very small potential gradient which exist in the atmosphere above 20 km indicate that the air at these levels is highly conducting.

WILSON (1922), who suggested that the origin of the fineweather electric field lay in thunderstorms, pointed out that, in consequence, its maximum value should occur when the most thundery regions of the earth attain their maximum activity. WHIPPLE (1929) found apparent correspondence between the variation in thunderstorm activity over the whole globe on average day and the variation of potential gradient as measured over the oceans and in the Arctic and Antarctic. There appears to be no appreciable annual variation of the potential gradient over the sea, but land stations in both hemispheres report a maximum in the local winter and a minimum in the summer.

The lower atmosphere is slightly conducting due to the existence of ions produced by radio-active matter in the air and in the earth, and by cosmic rays. The space-charge density  $\rho$  decreases with height in conformity with equation (3.2) and the variation of the potential gradient with height. The positive space charge results from an excess of positive ions which on average, balance the negative charge on the Earth's surface. The ions may be divided into two groups: small ions, and large ions. The concentrations of positive and negative ions are not very different, but there is a small excess of positive ions representing the positive space charge; the ratio of the concentration of the small positive and negative ions is about 1.2.

The electrical conductivity of the air which is proportional to the product of the concentration and mobility of the ions, increases quite rapidly with height up to about 20 km. The conductivity of the atmosphere is slightly greater for positive than for negative ions.

The drift of the positive ions downwards and of the negative ions upwards under the fine-weather field, constitute a downwardly directed conduction current which tends to neutralize the Earth's negative bound charge. The current  $i$  flowing through unit area normal to the field is given by

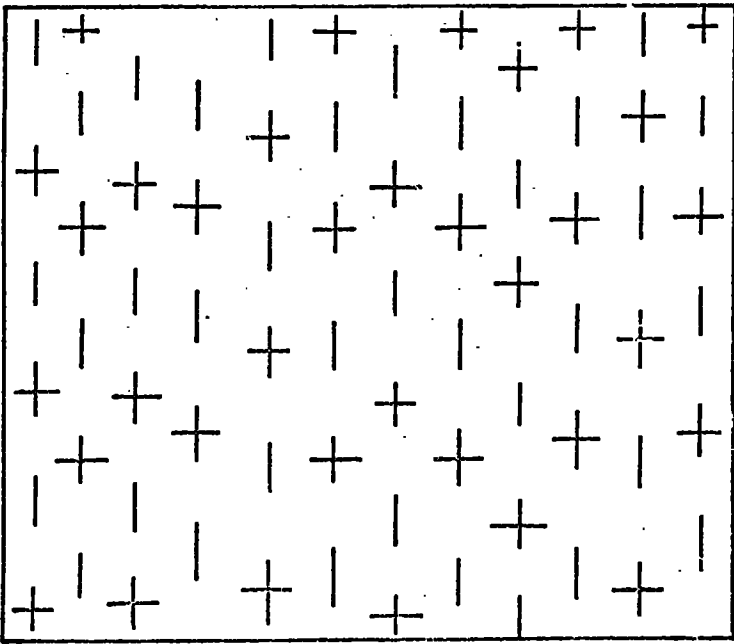
$$i = F(\lambda_+ + \lambda_-) = Fe(n_+k_+ + n_-k_- + N_+K_+ + N_-K_-)$$

where  $\lambda_+$  and  $\lambda_-$  are the polar conductivities,  $k, K$  the ionic mobilities of small and large ions respectively,  $n, N$  the ionic concentrations, and  $e$  the ionic charge. The magnitude of the fine weather current density is generally taken to be about  $2 \times 10^{-12}$  A m<sup>-2</sup> over land and  $4 \times 10^{-12}$  A m<sup>-2</sup> over the sea, though recent measurements may show that these values will have to be revised. The increase of  $\lambda$  with height is offset by the decrease of  $F$ , so that the current is almost independent of height.

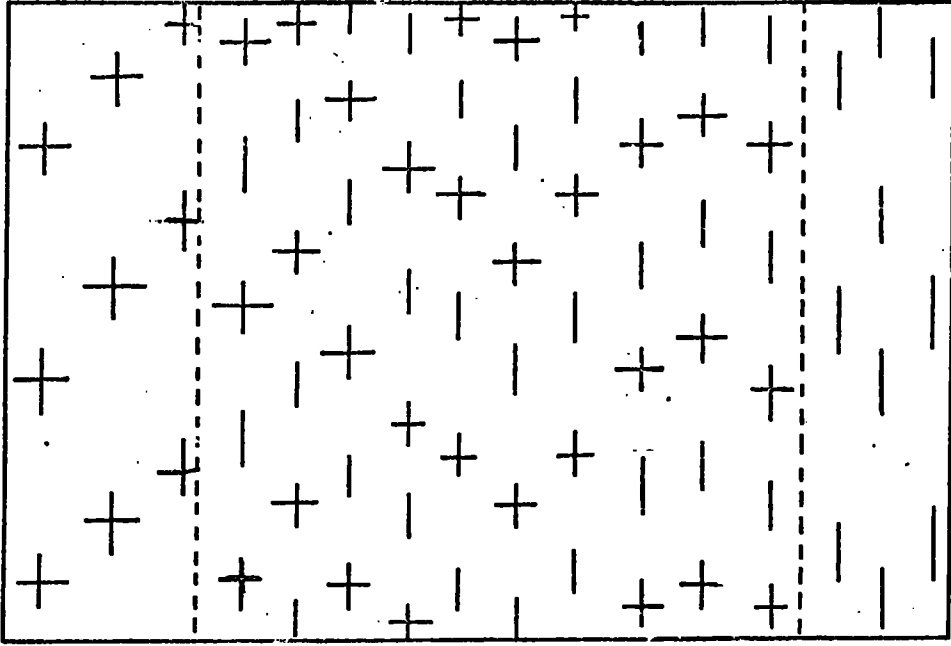
Measurements of the variation of conductivity with height during balloon ascents allow the resistance of a unit column of the atmosphere, cross-sectional area m<sup>-2</sup>, to be calculated. GISH and SHERMAN (1936) deduce from their results a value of  $10^{19}$   $\Omega$ , the resistance of the whole atmosphere thus being about  $2 \Omega$ .

### 3.2 Charge generation in clouds

Polarization of the cloud in the requisite direction follows automatically by the action of gravity in pulling the negative charges down Fig.3.2; When an updraught in the cloud is capable of supporting or even of driving upwards the heavier negative group of carriers, raindrops or



(a)



(b)

Fig.3.2 Gravitational Separation of opposite charges. (After WILSON).

snow or large ice-particles, the lighter ones, droplet or ice-fragments, are driven upwards still faster, so that the relative velocity of separation of the two groups is the same as if no updraught were present.

The shape of the field-changes immediately after a cloud discharge suggests that the process of separation of the oppositely-charged carriers is one involving initially free fall under gravity and that this free fall is progressively retarded and finally reduced to nearly zero by the attractive forces between the separating charges. The rate of fall of the heavier carriers in this final stage must be considered just sufficient to maintain the charges constant in the face of dissipation currents within the cloud and directed to it from outside. Ultimately the field between the separated charges may become strong enough for a discharge to pass. If the charges are equal, this leaves the cloud in its initial state and the larger carriers in the neutral region of Fig.3.2 once more separate and under the action of gravity. The relative velocity of separation has been taken by WILSON (1929) to be of the order of  $6 \text{ ms}^{-1}$ , the terminal velocity of a water drop 1.5 mm in radius. Relative to such a drop, the much slower positive droplets may be considered as stationary. WILSON has examined the case of a disc-shaped region of charge-generation (Fig.3.2) making use of his measurements of the average moment  $M$  developed before discharge and  $dM/dt$  just after discharge. He has assumed the thickness of the disc to be about 1 km and the discharge to occur when the field reaches  $10^6 \text{ V m}^{-1}$ . From this information he found that (a) the volume of the generating region is  $4 \text{ km}^3$  and hence its cross-section  $4 \text{ km}^2$ ; (b) the rate of generation of charge is equivalent to about  $1 \text{ A km}^{-2}$  of surface and is therefore about  $4\text{A}$  in all; (c) the total charge or either the positive or the negative carriers in the neutral generating region is about 500 C; (d) the charge per c.c. on the larger carriers is of the order of, but should not exceed, 30 e.s.u. .

A different type of cloud polarization by gravity has been discussed by FRENKEL (1947) in connection with fog-like clouds of small droplets. These are considered by him to be capable of capturing negative ions from the air which is then left with an excess positive charge. The charged droplets are not held up completely by the internal field but drift slowly downwards at such a rate that the polarization charge developed per unit area is equal to the charge neutralised by the internal conduction or dissipation current in the same time. The internal field,  $E_s$ , in this "stationary" condition is related to the equilibrium field  $E_q$  in which the drops are fully supported by the equation  $E_s/E_q = \Delta/\lambda$  where  $\lambda$  is the ionic conductivity of the air and  $\Delta$  is the much smaller contribution to the conductivity provided by the droplets, then  $E_s$  is found to be of the order of  $10^4$  V m<sup>-1</sup>, hundred times less than  $E_q$ . In clouds where the water content is greater, the positive ions will attach themselves to larger particles and the development of polarization in the thundercloud then appears to become the same as that considered by WILSON (1929).

### 3.3 Lightning

The most frequent form of lightning is the cloud discharge. Though most cloud flashes are known from field-change records to occur between the main P (positive) and N (negative) charges of the cloud dipole, there is evidence that others pass between the N charge and a lower positive charge, either the small p pocket of Fig.3.3, N-p discharge, or a positive space-charge in the air below the cloud (air-discharge). A similar type of flash between the P charge and negative charge drawn down from the upper air to the top of the cloud or to the air immediately above it, would account for many cloud-flashes which are seen at night to be restricted to the cumulus heads of thunderclouds and the regions above them.

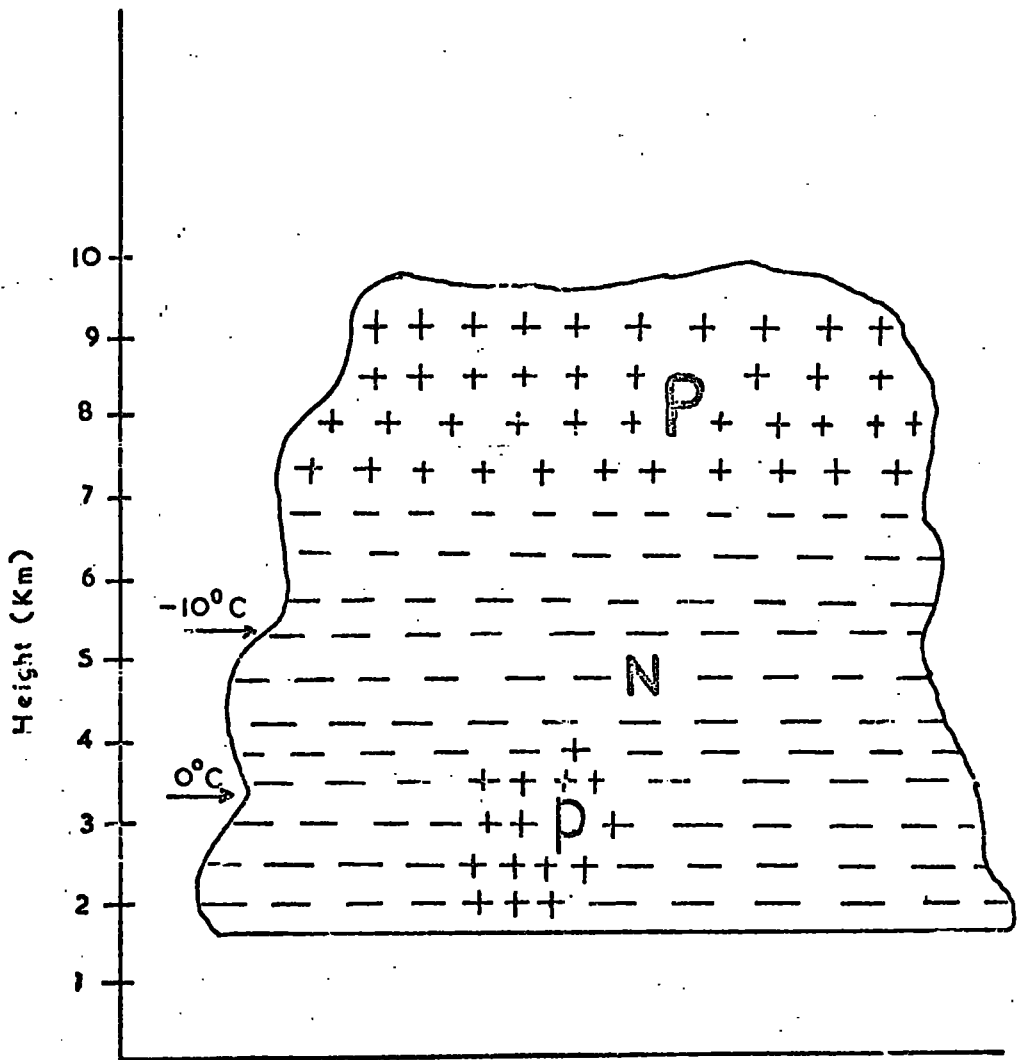


Fig.3.3 The distribution of charges in thunderclouds. (After SIMPSON, SCRASE and ROBINSON).

Most ground-discharges remove negative charge from the N region. There is a good deal of evidence to show that they are usually triggered off by the strong field between the N and p charges or the positive space-charge in the air, thus extending an N-p or an air discharge all the way to the ground. The residue of the negative charge remains after the small lower positive charge has been neutralised. Many lightning flashes, both within the cloud and to ground are observed to flicker. Early camera studies showed that this is due to the fact that the discharge consists of a number of separate components or strokes. Though the whole flash often occupies more than a second, the luminosity of the component strokes is generally over in a few milliseconds. After each stroke the ionisation along its channel, though much reduced by electron-attachment and by recombination and diffusion of the ions, usually persists in sufficient measure to provide the following stroke with a ready-made path which it follows. If, however, the time-interval is exceptionally long, the channel ionisation is too much weakened and the following stroke may take a different path.

The channel is often shifted several meters by the wind in the intervals between strokes; the discontinuous nature of the discharge is then shown as ribbon lightning. Observations with moving cameras show that the branching of the lightning discharge to ground is almost always confined to the first stroke of a series. The maximum number of strokes so far observed from a single flash to ground is 42. The most frequent number is 3 or 4 and single-stroke discharges are quite common. The time-interval between strokes is variable, the most frequent value lying between 30 ms and 70 ms.

#### 3.4 Electrical and meteorological conditions inside thunderclouds

An investigation of the electrical and meteorological conditions inside thunderclouds was started in 1945 at the Zugspitze Observatory in

Germany. During a three years period 125 storms, consisting of 67 thunderstorms and 58 shower clouds with high electric fields, were analysed with regard to (a) electrical conditions, (b) precipitation, and (c) miscellaneous meteorological details. The more important aspects of the results may be summarized as follows:

1. The average field direction at different temperature levels of the cloud, Fig.3.4, confirms the opinion of SIMPSON and ROBINSON (1941); In the active parts of a thundercloud, there are generally three main charges - a local positive charge in the base, a negative charge in the lower part, and a positive charge in the upper part.
2. The average positions of these charges may be specified as follows:
  - (a) The centre of the local positive charge in the lower cloud is accurately fixed near the freezing level. This charge seems to have a horizontal extent of less than 1 km, placed in the centre of precipitation and lightning.
  - (b) The main negative charge is concentrated. on the average, near the  $-8^{\circ}\text{C}$  level and occupies a larger area than the lower positive charge, in the vertical as well as in the horizontal direction.
  - (c) With regard to the main positive charge, its position was found to be higher than the negative charge and its area to be quite extensive. These charge positions are mean values of a great number of thunderclouds. In each case, there may be great local and temporary variations.
3. The centres of the local positive charge in the cloud base and of the negative charge above are probably bound to the same vertical air column, lightning-precipitation-downdraft centre, while the centre of the high positive charge is located outside this air current, following at a distance somewhat behind it. The negative

$\oplus \ominus$  = SPACE CHARGES (SIGN)  
 + - = POTENTIAL GRADIENT (SIGN)  
 $\circ$ — $\circ$  = LINES OF ZERO FIELD STRENGTH

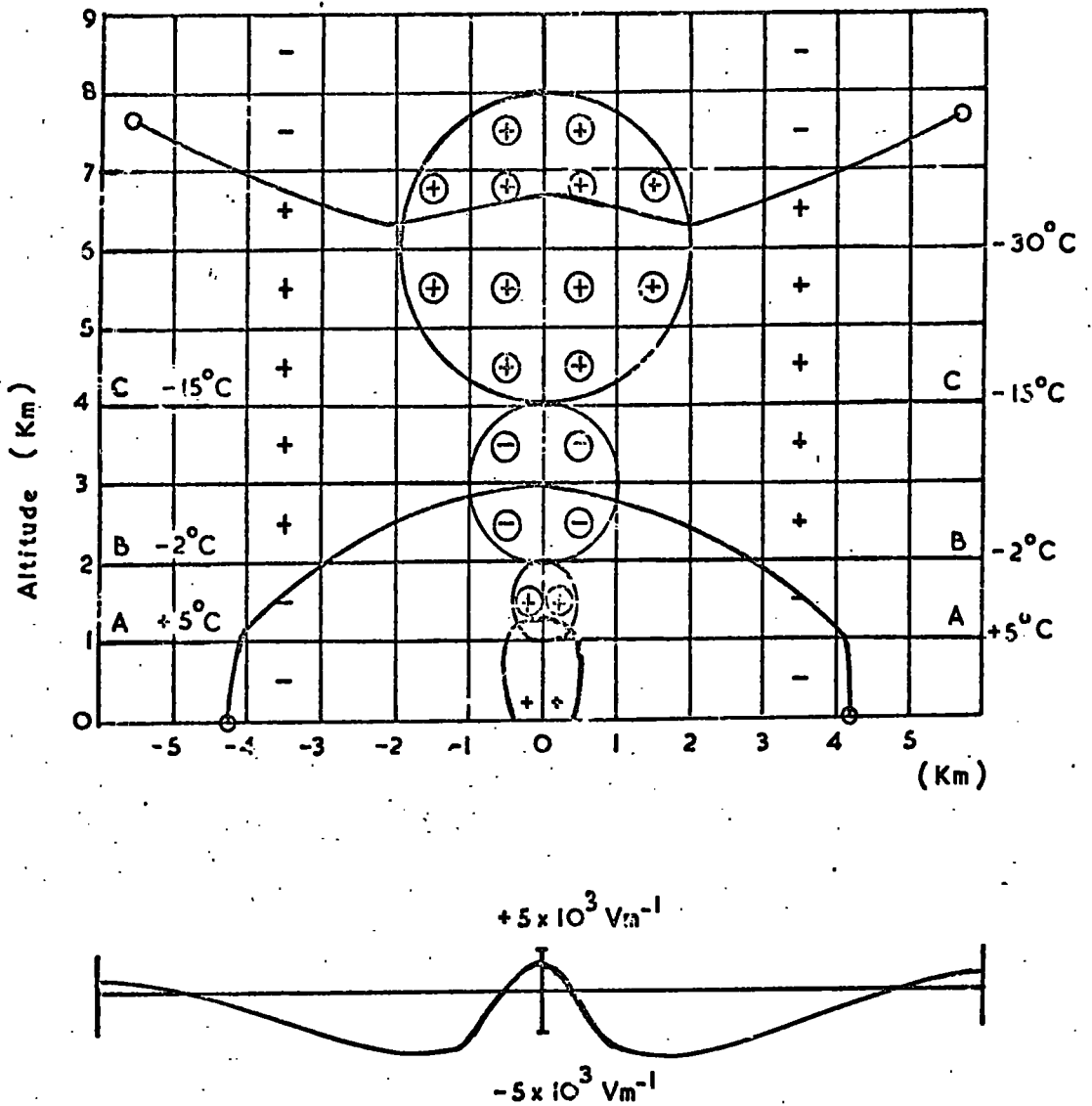


Fig.3.4 Distribution of electric space charges and variation of vertical potential gradient at ground (lower curve).  
 [After SIMPSON, SCRASE and ROBINSON].

- charge centre is apparently the starting point of most lightning.
4. The two main space charges are generally held within the limits of the clouds, not in the free air or in the precipitation area below the clouds.
  5. No fundamental difference could be found between thunderstorms and snow-showers cloud without lightning. They have a similar electrical structure if they are compared at the same temperature level; a winter snow-shower cloud, although it contains less liquid water, may be considered as a pseudo-thundercloud whose lower parts are cut off by the cloud base or the ground.
  6. Cumulus clouds with precipitation but without lightning, shower clouds, have a field strength comparable to that of thunderstorms, even if their vertical extent is smaller. Cumulus clouds without precipitation never show a field strength comparable to thunderclouds, even if their vertical extent and liquid water content are very large FRENKEL (1944-1947).
  7. There is no fundamental electrical distinction between local convective and frontal storms, the main difference being in their flow pattern.
  8. The records of the electrical and meteorological elements show variations and oscillations with periods on the order of minutes. Taking into account the observed wind velocities, this indicates that the individual cells in a thunderstorm, which are about 1 to 10 km in linear dimensions, are further sub-divided into units of order of magnitude 0.1 to 1 km. This "parcel structure" applies also to the main electrical charges. It may be related to turbulence systems and gives some indication of the notorious local character of breakdown fields and of intricate composition of thunderstorms.

### 3.5 The electrical structure of thunderstorms

Although it is now over two hundred years since the electrical nature of the thundercloud was firmly established by the experiments of FRANKLIN (1752) and D'ALIBARD (1752), the electrical mechanisms responsible for the charging of the cloud are still not understood. By measuring the electrical field intensity due to both near and distant clouds, SCHONLAND (1928), WORMELL (1939), MALAN and SCHONLAND (1950) and SMITH (1954) have established the approximate magnitudes and relative positions of the main charge centres. Similar information was obtained by APPLETON et al. (1926), WORMELL (1939), MALAN and SCHONLAND (1951) and PIERCE (1955), by measuring the electric field charges brought about by lightning flashes. Simultaneous multiple-station recording of potential gradient and other parameters has enabled WORKMAN et al. (1942), BARNARD (1951) and REYNOLDS and NEILL (1955) to estimate more accurately the magnitude of the charge centres and their positions relative to the cloud. Aircraft and balloon measurements have also produced useful information, particularly those of SIMPSON and SCRASE (1937), SIMPSON and ROBINSON (1940) and GUNN (1948).

The generalised electrical structure obtained from these measurements is an approximate double dipole, with the upper cloud charges being positive, the main lower charges being negative, and with a second positive charge of smaller magnitude Fig.3.5 .

Earlier workers assumed the main charge centres to be distributed vertically above one another, but the measurements of PIERCE (1955) and BROOK (1969) suggest that considerable horizontal separation of charge centres may exist. Estimates of the quantities of charge involved vary considerably, but the excess charges in the main charge centres must be at least several tens of Coulombs. The main negative and positive charge centres in the thunderclouds of temperate latitudes exist at temperatures

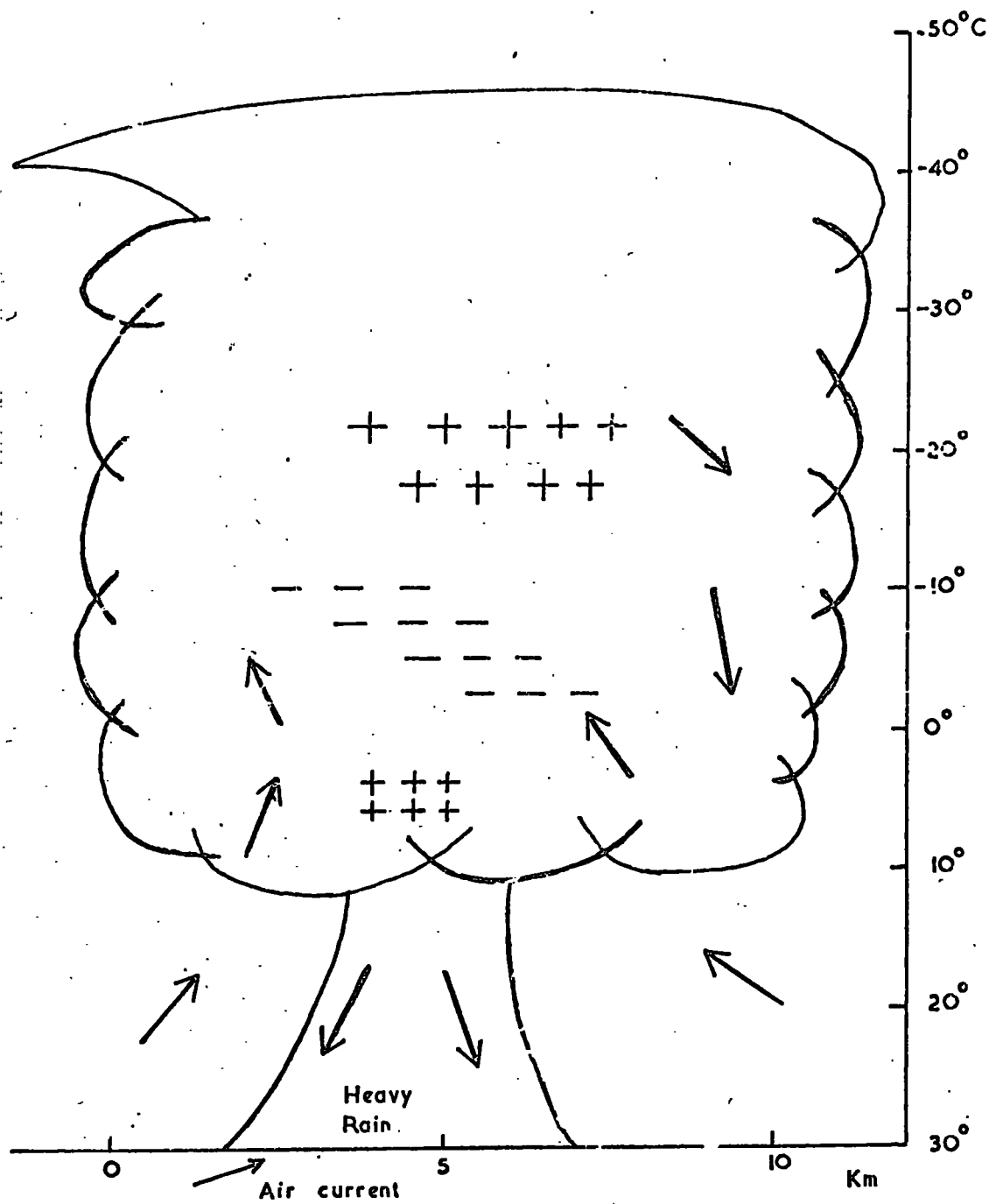


Fig.3.5 Location of main thunderstorm charges.

below freezing, in regions where both solid and liquid hydrometeors exist, and the most favoured charging theories involve gravitational separation of oppositely charged particles, with the main updraught carrying the smaller particles aloft.

Examination of the recovery curve of potential gradient after lightning discharges has shown that regenerative currents of several amperes per storm cell are perhaps necessary. Aircraft measurements by GISH and WAIT (1959) have shown that conduction currents of this magnitude flowing to the ionosphere do exist. The potential gradient at the ground beneath a storm reaches a maximum value of around  $10,000 \text{ V m}^{-1}$ , being limited by a space charge blanket of opposite sign released by point-discharge from raised objects. Precipitation current densities at the ground are found to be extremely variable in sign and magnitude, maximum values being of the order of  $0.1 \mu\text{A m}^{-2}$ . It should be noted that this value is at least two orders of magnitude too small to explain the observed charges in the cloud, and it is generally thought that the charges on precipitation particles are much larger in the cloud. The most active thunderstorm cells produce flashes at a rate not normally exceeding one every five seconds, so that any theory of electrification must be able to explain these high rates of charge production.

## CHAPTER 4

### NIMBOSTRATUS CLOUDS

#### 4.1 Introduction

Nimbostratus clouds are both of considerable vertical height and horizontal extent. They give rain although usually less intense than that from cumulonimbus. Nimbostratus clouds are formed when moist warm air rises over a denser mass of cold air at a warm front as shown in Fig.4.1. They have a smaller vertical air current and is less turbulent than the cumulonimbus cloud. Because of these differences it is described separately here.

#### 4.2 The electrical structure of nimbostratus clouds

CHALMERS (1959) considers the nimbostratus clouds as being of sufficient horizontal dimensions to render the edge effects negligible. The quasi-steady state, which may be assumed to be reached in a nimbostratus system, implies that the total vertical current density is independent of height. The components of the total vertical current density is independent of height. The components of the total current, namely precipitation, conduction and convection currents, vary in their contribution with height, (e.g. the total current will be comprised completely of the conduction current above the cloud).

Although an analytical solution of the general problem is impossible, CHALMERS has worked out two limiting cases for both rain and snow clouds between which the true solutions are likely to lie. The results of CHALMERS analysis for rain clouds, which is reproduced in Fig.4.2, was a vertical profile of potential. Since the rain began as snow which is usually negative there must be a process of charging at or below the melting level to give the positive rain current usually observed e.g. CHALMERS (1956). The

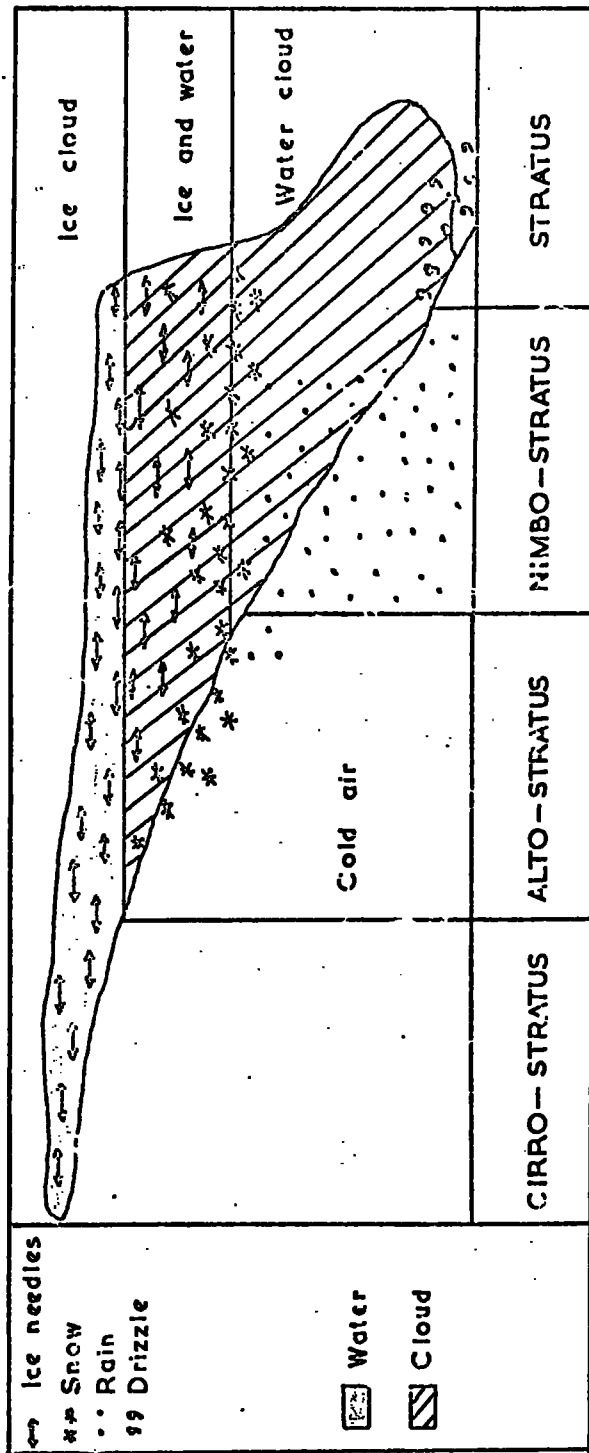


Fig.4.1 Clouds formed at a warm front.

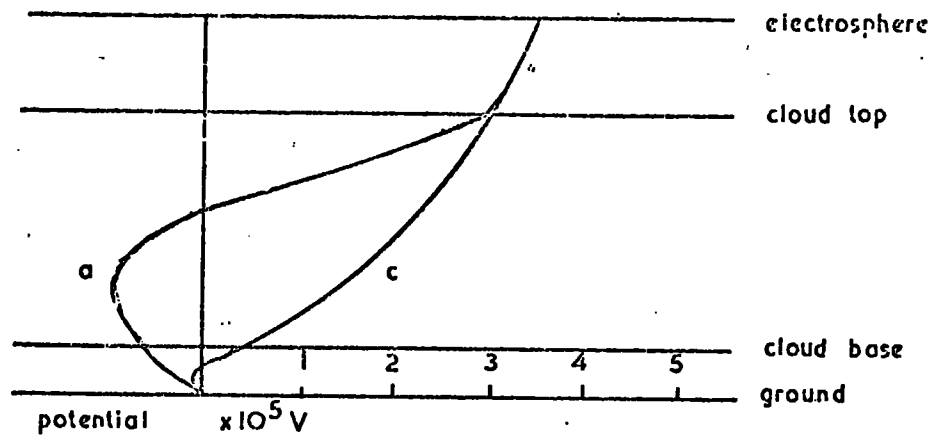


Fig.4.2 Vertical profiles in nimbostratus. (After CHALMERS).

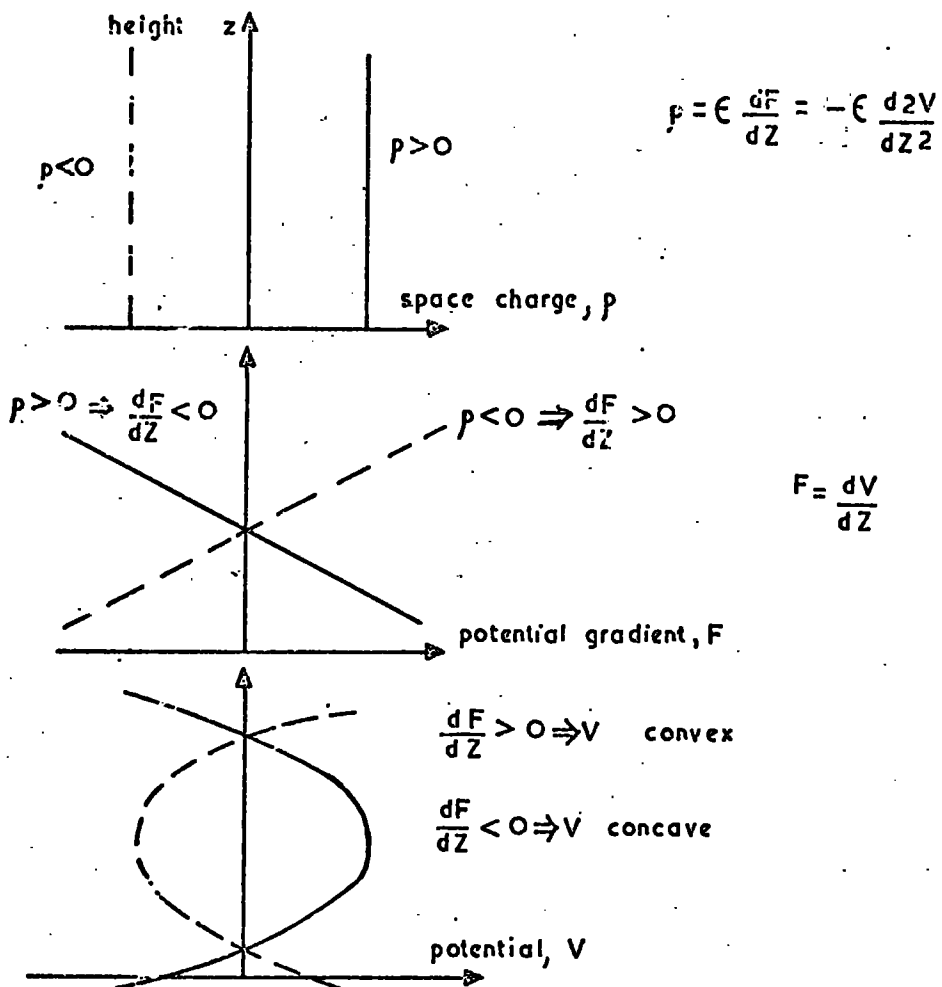


Fig.4.3 Vertical profiles of  $V$ ,  $F$  and  $\rho$ .

negative space charge liberated in such a separation accounts for the negative potential peak shown in the profile. The profile (c) is for the case where the charge separation takes place at or near the ground by, as SMITH (1955) suggests, splashing for example. Profile (a) is for the case where the separation takes place above the cloud base.

CHALMERS believes that (c) is less likely than (a) to be near the true state of affairs because the space charge in the cloud is known to be everywhere negative. A negative space charge requires that the profile should be convex, viewed from the left, as a simple quantitative examination, Fig.4.3, of Poisson's equation shows. Hence it can be seen that (a) satisfies the requirement where (c) does not.

#### 4.3 A proposed model for nimbostratus clouds

Instead of including the clouds in the earth ionosphere current network, it is proposed by STRINGFELLOW (1969) that we can consider the cloud charges to be independent of outside electrical effects. It was assumed that any ionic or cloud space charges dissipate only by ionic conduction, and that the rate of dissipation of these charges depends only on their magnitude and the conductivity in the immediate environment. It was further assumed that any charge separation process gives rise to an ionic or cloud charge and a precipitation charge of opposite sign.

The charged precipitation was then assumed to fall to the ground, and the total precipitation current at the ground was considered to represent the total current flowing downwards from the charging region.

It was suggested that, if we know the horizontal and vertical dimensions of the cloud system, and if we can measure the precipitation current density, then we can calculate the value of the cloud ionic charge, and hence its contribution  $F_p$  to the potential gradient at the ground. In order

to calculate the potential gradient at the ground due to the whole system, we must take into account the space charge on the falling precipitation. If the contribution to the potential gradient at the ground due to the precipitation space charge is  $F_s$ , then the total potential gradient at the ground is given by

$$F = F_\rho + F_s \quad (4.1)$$

#### 4.3.1 The general case

For steady conditions, if we consider a cylindrical cloud zone of depth  $H$ , radius  $R$  and cloud base height  $h$  Fig.4.4, then if precipitation with uniform current density  $I$  is leaving the cloud base, the total precipitation current leaving the cloud is  $\pi R^2 I$ . If the cloud charge density at any time is  $\rho$ , the total cloud charge will be  $\pi R^2 H \rho$ , and the ionic conduction current out of the cloud region will be  $(\pi R^2 H \rho) \lambda / \epsilon_0$ . Thus the total current out of the cloud zone will be  $\pi R^2 I + (\pi R^2 H \rho \lambda / \epsilon_0)$ . This is equal to the rate of decrease of cloud charge,  $-\frac{d}{dt} (\pi R^2 H \rho)$ , which is then given by

$$-\frac{d}{dt} (\pi R^2 H \rho) = \pi R^2 I + \pi R^2 H \rho \lambda / \epsilon_0$$

Thus the rate of accumulation of cloud charge density in the cloud zone is given by

$$H \frac{d\rho}{dt} = -I - \frac{H\rho}{\tau} \quad (4.2)$$

where  $\tau$  is the relaxation time ( $\epsilon_0 / \lambda$ ) in the cloud.

The potential gradient at any point due to the cloud charges can be obtained by integrating over the cloud volume. The potential gradient at the ground under the centre of the cylinder is found to be given by

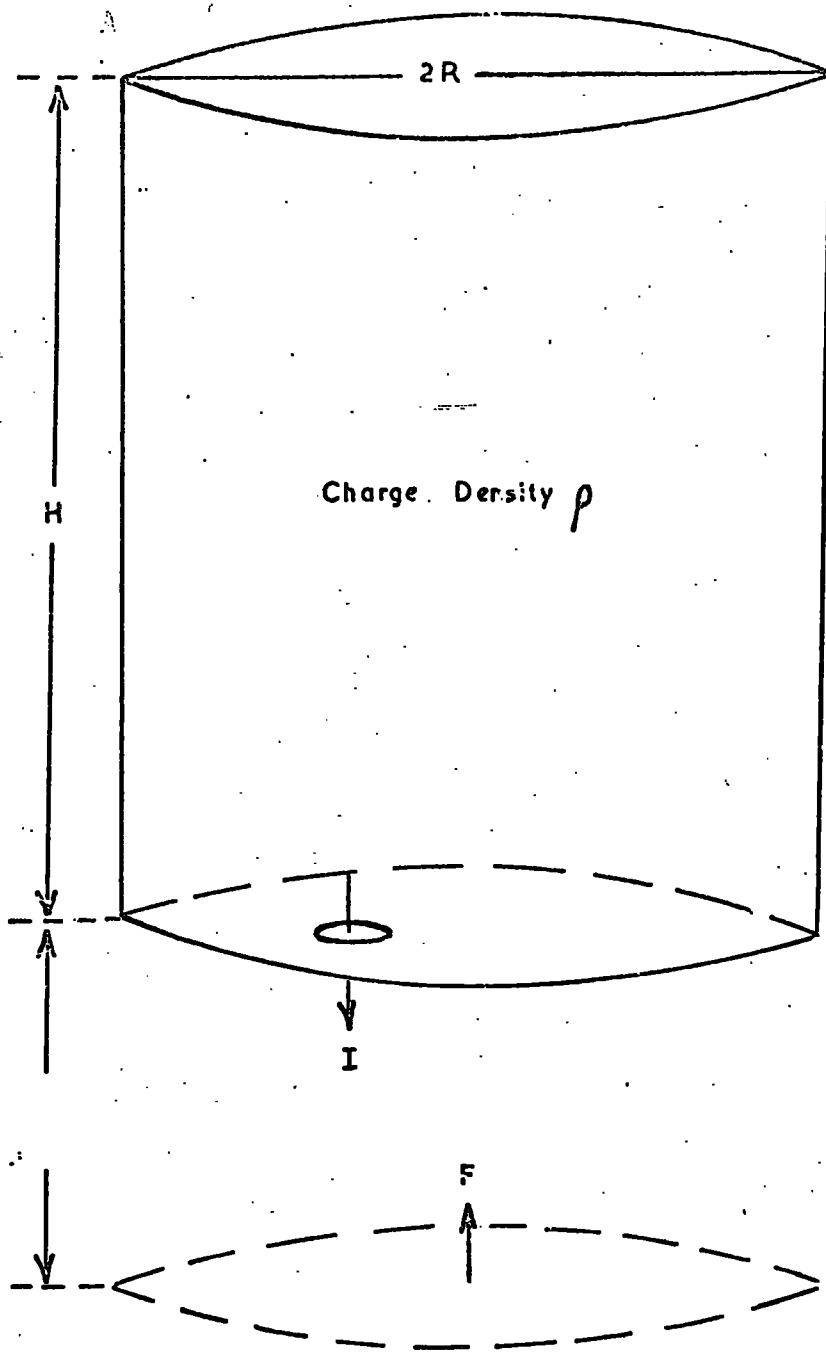


Fig.4.4 Cylindrical cloud model. (After STRINGFELLOW).

$$F_{\rho} = \frac{\rho}{\epsilon_0} \{H - \sqrt{(H+h)^2 + R^2} + \sqrt{(h^2 + R^2)}\} \quad (4.3)$$

If R is very large compared with H and h, the potential gradient at the ground due to the cloud charges is then given by

$$F_{\rho} = \frac{\rho H}{\epsilon_0} \quad (4.4)$$

In order that a charge separation process should produce a cloud charge density uniform with height, it is necessary that the precipitation current density should increase linearly with decreasing height throughout the charging region. If the precipitation obtains its charge uniformly throughout the depth H, and then falls through height h to the ground without charge loss, then the potential gradient at the ground under the cloud centre due to the precipitation space charge is found by integration to be given by

$$F_z = \frac{I}{2\epsilon_0 V} \left\{ H + 2h + 2R + \frac{h}{H} \sqrt{h^2 + R^2} - \left(1 + \frac{h}{H}\right) \sqrt{(H+h)^2 + R^2} - \frac{R^2}{H} \log \frac{(H+h + \sqrt{(H+h)^2 + R^2})}{(h + \sqrt{h^2 + R^2})} \right\} \quad (4.5)$$

If R is very large compared with H and h, the contribution to the potential gradient at the ground by the precipitation space charge is given by

$$F_s = \frac{I}{2\epsilon_0 V} (H + 2h) \quad (4.6)$$

Thus if we know the precipitation current density, the conductivity of the cloud, and the dimensions of the charging region, it is possible to calculate the potential gradient at the ground due to the charge system.

This model is of necessity oversimplified. Charged cloud systems would be expected to interact electrically with each other, and the existence of

wind shear and precipitation particles of different sizes will also complicate matters. However, provided the precipitation current density is greater than the ionic conduction current density to ground, and provided the potential gradient is not sufficiently high to give point discharge near the ground, then this model is perhaps a fair representation of conditions.

#### 4.4 Relation between precipitation current and potential gradient

There exists during continuous rain a general inverse relationship of positive precipitation current and negative potential gradient.

The inverse relation is not always observed, but this can possibly be explained by considering the type of collector used. If the shielding on the collector is too great it will prevent the majority of small drops, which are found to carry a charge of opposite sign to the potential gradient, entering the collector. SMITH (1955) measured the charge on a large number of drops during a short time interval and found that the sum of the charges on the drops was of the same sign as the potential gradient. But he found that if he used the same apparatus as SIMPSON (1949) he obtained the inverse relation as obtained by SIMPSON. In his original experiment SMITH was unable to measure the charge on small drops due to the limitations of his apparatus. This would suggest that the inverse relation is mainly due to the smallest drops.

SIMPSON (1949) observed that the variation of precipitation current and point discharge current with time often appear almost to be the mirror image of each other. But SIVARAMAKRISHNAN (1951) found that the change of sign of the precipitation current synchronises more closely with the change of sign of the potential gradient than with the point discharge current. It is this latter effect that will be referred to as the mirror image effect.

During periods of continuous rain the potential gradient is not usually

large enough for point discharge, and RAMSAY and CHALMERS (1960) found that the positive maximum of the precipitation current often led or lagged behind the negative maximum of the potential gradient by a few minutes. SIMPSON (1949) also observed that the mirror was not the zero value of potential gradient but corresponded approximately to the normal fine weather value.

As a drop takes a few minutes to fall from the cloud to the ground the existence of the mirror image effect would suggest that the drops acquire their charge close to the ground and so that the charging of the rain is not due to the theory of WILSON (1929) as the potential gradient would be too low. But CHALMERS (1957) suggested that the mirror image effect could be explained by considering the motion over the observer of clouds carrying different charges at different places rather than due to changes in the cloud. This would allow the mirror image effect to be observed no matter at what height the drop acquires its charge, and so the drops could still obtain their charge according to the WILSON influence theory in the larger potential gradient at higher levels.

MAGONO and ORIKASA (1960) and (1961) found that occasions when the mirror image effect did not hold could possibly be explained by considering the space charge due to the charge on the rain itself. They said that the mirror image effect could be explained by considering the removal from the cloud of charge of one sign and the leaving behind of charge of the opposite sign in the cloud. So any change in the rate of rainfall would result in a change of the space charge due to the drops and cause a temporary change in the potential gradient at the ground.

STRINGFELLOW (1969) suggested that looking upon the potential gradient as a fundamental characteristic of the cloud and the precipitation current as a secondary effect is physically the wrong way round, and that they are both the result of a single cause, namely charge separation in the cloud.

The whole system of charges then gives rise to the potential gradient at the ground, which should therefore be regarded as a dependent not independent, variable.

## CHAPTER 5

### A SURVEY OF PREVIOUS WORK ON CLOUD DROPLET ELECTRIFICATION

#### 5.1 Introduction

A number of the basic problems of modern atmospheric physics are related to the electrical charges normally observed on cloud droplets, dust, and rain. The origin of this electrification has been obscure and the magnitude and distribution of the charges uncertain. It is well established that many solid dusts dispersed in the atmosphere are highly electrified and that this electrification plays some part in determining the effective coagulation rates. It has been surmised that cloud droplets have similar properties. However, the frictional contact usually invoked to describe the origin of charges on solid dusts does not appear applicable to cloud droplets, and appeal to direct measurement is required.

#### 5.2 Work in the period up to 1946

As early as 1911, MILLIKAN made significant observations that apply directly to the problem of droplet charging by ionic diffusion. While watching droplets acted on both by gravity and by a vertical electric field, he observed that "even when the drop had a negative charge of from 12 to 17 units, it was not only able to catch more negative ions but it apparently had an even larger tendency to catch the negative than the positives. Here, then, is an absolutely directed proof that the ion must be endowed with a kinetic energy of agitation, which is sufficient to put it up to the surface of the drop against the electrostatic repulsion of the charge on the drop". He further concluded from his data that the only way a droplet could lose or gain charge was to capture an ion of appropriate sign. It is a fair inference from MILLIKAN'S measurements that the diffusion of ions onto

droplets is a real and continuous process, and that ions, once captured by a droplet, can never escape because of the work they must do to overcome the image forces. Calculations show that the image force is appreciable for a distance of considerably less than one free path away from the surface of the droplet. Therefore, ion capture by a free surface is relatively insensitive to the character or dielectric constant of the drop, and image forces in the surrounding air play a relatively minor role. The possibility of selective absorption due to quasi-crystalline double layers at the surface of the droplet is specifically neglected in this investigation.

Attempts have been made to formulate quantitatively the charging of spherical droplets, and some measurements on droplets of cloud size have been made. For example, ARNDT and KALLMANN (1925) have made measurements on droplets composed of paraffin oil in the presence of large numbers of ions of one sign. They found rather large charges on their droplets and worked out an approximate theory for the equilibrium values on the assumption that only one type of ion was present. Much later, FRENKEL (1946) attempted to work out a better approximation that considered the effects when both positive and negative ions were present. Unfortunately, he imposed boundary conditions of doubtful reality, and his results have limited applicability.

### 5.3 GUNN 1947-1955

The electromechanics of droplet electrification were investigated. He shows that the atmospheric ions formed by cosmic rays or other means normally diffuse onto cloud droplets and electrify them. Two basic types of droplet electrification by ionic diffusion are recognized.

Systematic electrification processes transfer free charges of one sign to most of the droplets. This occurs whenever the product of ionic density

and mobility of one type of ion notably exceeds that of the other. Superimposed upon this kind of electrification is statistical or random electrification. In this case, charge are transferred to droplets by diffusion and build up positive charges on some of the droplets and negative charges on others.

The systematic equilibrium-free charge  $\phi_0$  placed on a droplet by ionic diffusion is given by

$$\phi_0 = \left[ 1 + F(aVe/2\pi KT u)^{1/2} \right] \left[ (aKT/e \ln \left( \frac{\lambda_+}{\lambda_-} \right)) \right]$$

where  $F$  is a dimensionless factor approximating unity,  $K$  the Boltzmann constant,  $T$  the absolute temperature,  $e$  the electronic charge,  $a$  the drop radius,  $V$  its velocity with respect to its environment, and  $\lambda_+$  and  $\lambda_-$  are the positive and negative light-ion conductivities of the environment. The effective mobility  $u$  of the ions in the diffusing layer outside the drop is given by

$$u = (n_+ u_+ + n_- u_-) / (n_+ + n_-) \quad (5.1)$$

where  $n_+$  and  $n_-$  are positive and negative ionic densities, and  $u_+$  and  $u_-$  the positive and negative mobilities, respectively.

The distribution of the droplets is a Gaussian function of the charge and is given by

$$F_x = \frac{F_t e}{(2\pi aKT)^{1/2}} \times \exp \left\{ \frac{- \left[ x - (aKT/e^2) \ln (\lambda_+/\lambda_-) \right]^2}{2(aKT/e^2)} \right\} \quad (5.2)$$

where  $F_x$  is the number of droplets carrying  $x$  elementary charges, and  $F_t$  is the total number of droplets. This basic equation is plotted in Fig.5.1. He found that the mean charge on cloud droplets irrespective of sign, is given by

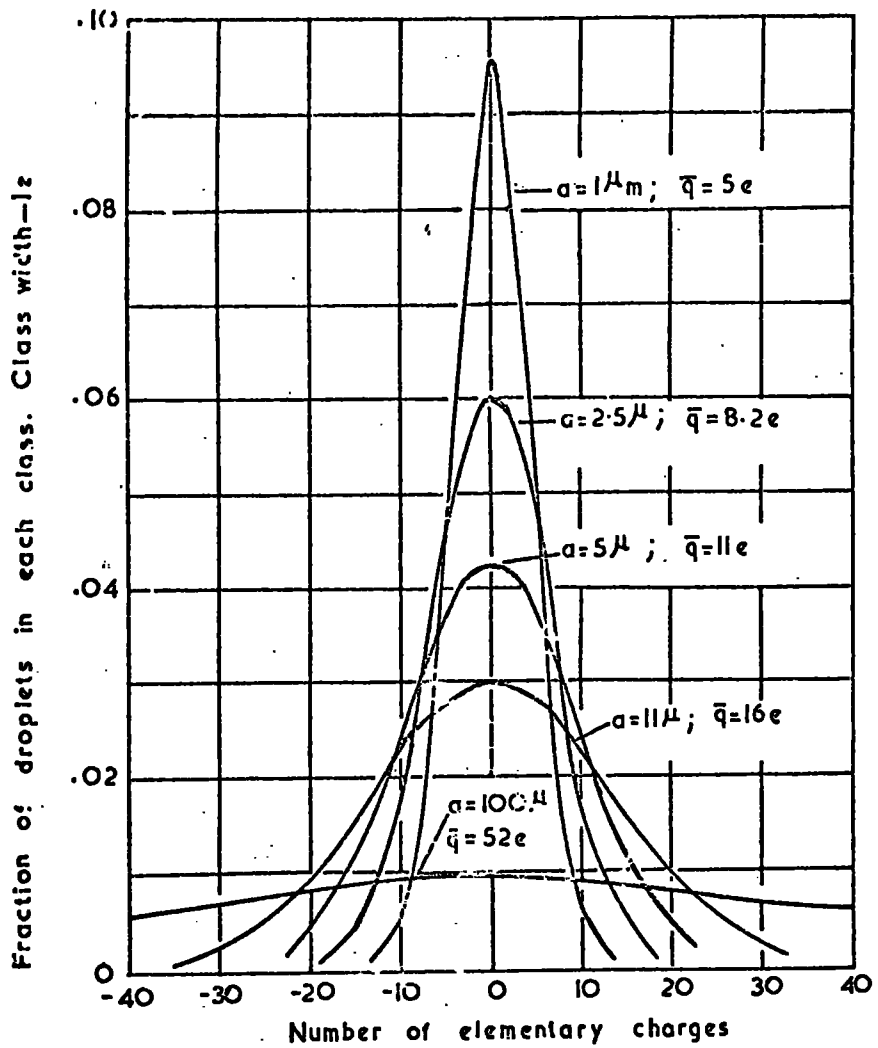


Fig.5.1. Distribution of fraction of total droplets carrying indicated number of elementary charges as calculated from (5.2). (After GUNN).

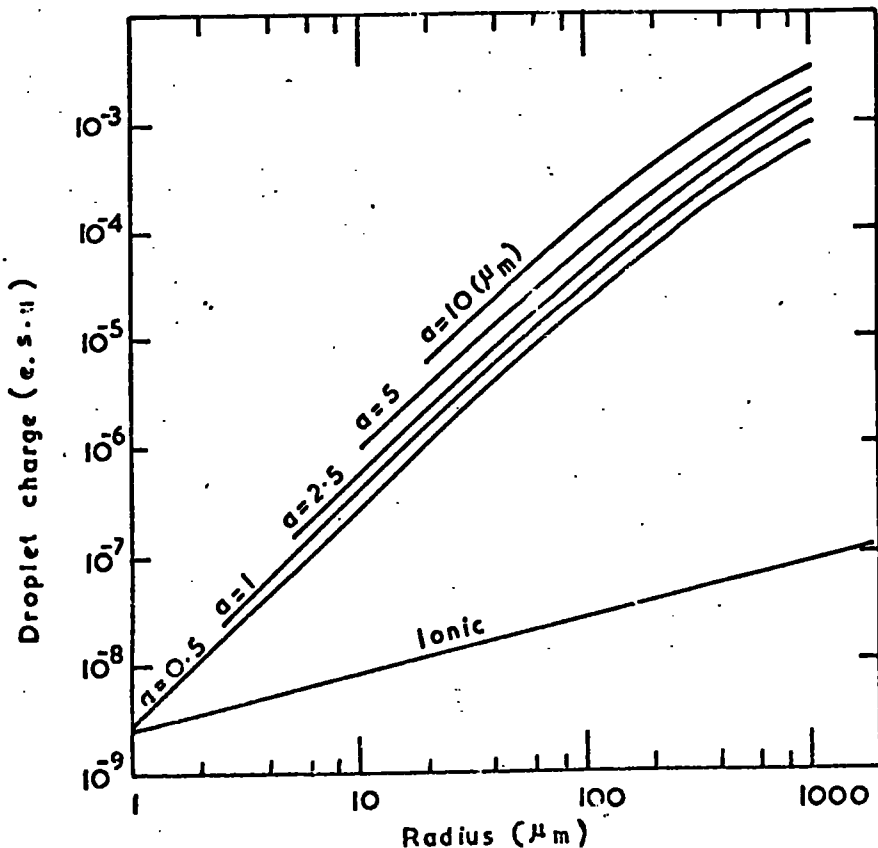


Fig.5.2. Mean charge, irrespective of sign, carried by associated droplets of radius given by abscissa when falling through droplets corresponding to indicated curve. Lower straight line "Ionic" is charge placed on droplets by thermal diffusion of ions. (After GUNN).

$$\bar{q}_+ = \bar{q}_- = \left( \frac{\pi n a k T}{2} \right)^{1/2} \quad (5.3)$$

The value of the expression is plotted in (Fig.5.2) and is marked "ionic". Recent measurements of the charges on some 250 laboratory-produced cloud droplets are displayed in (Fig.5.3). The free electrical charge on precipitation elements and the temperature, respectively, as functions of height are shown in (Fig.5.4). The measurements were made in the steady rain of a weak occluded front of the cold type. Only the larger drops, precipitation elements, and larger charges were measured. The number of drops carrying charges larger than 0.1 e.s.u. was relatively small. GUNN reports that the electrical field during these measurements did not exceed 2500 V m<sup>-1</sup>. The vertical distribution of charges is much the same as that of the thunderstorm, and in agreement with the distribution to be expected from a consideration of the proposed cloud-electrification hypothesis.

#### 5.4 SARTOR 1954

A laboratory experiment is described in which liquid drops are formed in a viscous medium to simulate cloud droplets in air by equating the Reynolde number for the experiment to that of the atmospheric case. Certain characteristics of the behaviour of drops of various liquids in different viscous media are described. Collision efficiencies and droplet trajectories differing markedly from previous theoretical calculations are presented for a limited number of drop sizes. The coalescence of water drops falling through mineral oil, and of water drops suspended in air, is found to depend on the strength of an applied electrical field.

With the aid of Fig.5.5, the drops in Fig.5.5a, under the influences of the external field, are polarized and have a potential difference  $E_0 c$  relative to each other. The drops are considered to be sufficiently close

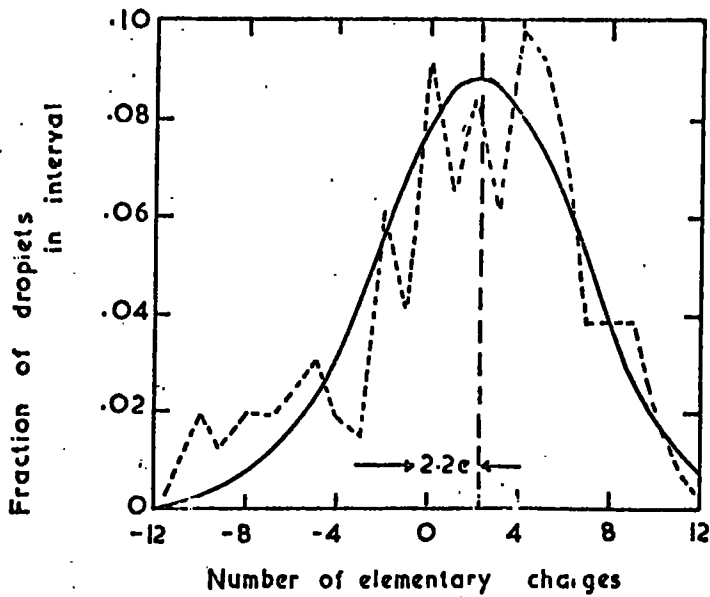


Fig.5.3 Observed fraction of cloud droplets carrying indicated numbers of elementary charges (dashed curve). Solid curve calculated from (5.2) with use of observed radius,  $a = 1.15 \mu\text{m}$ . (After GUNN).

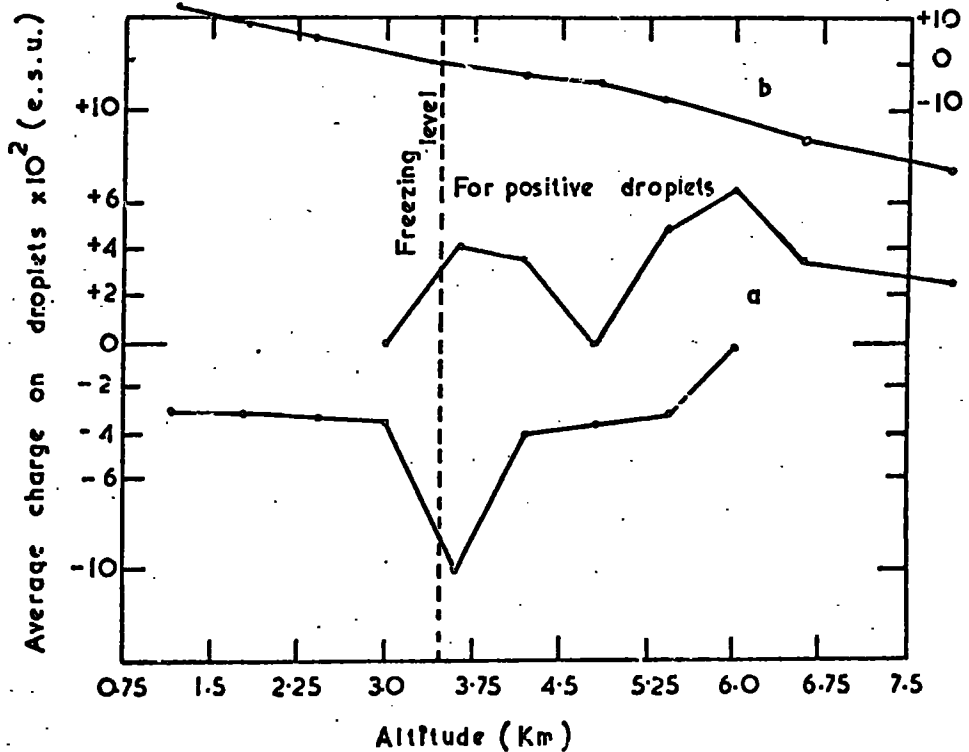
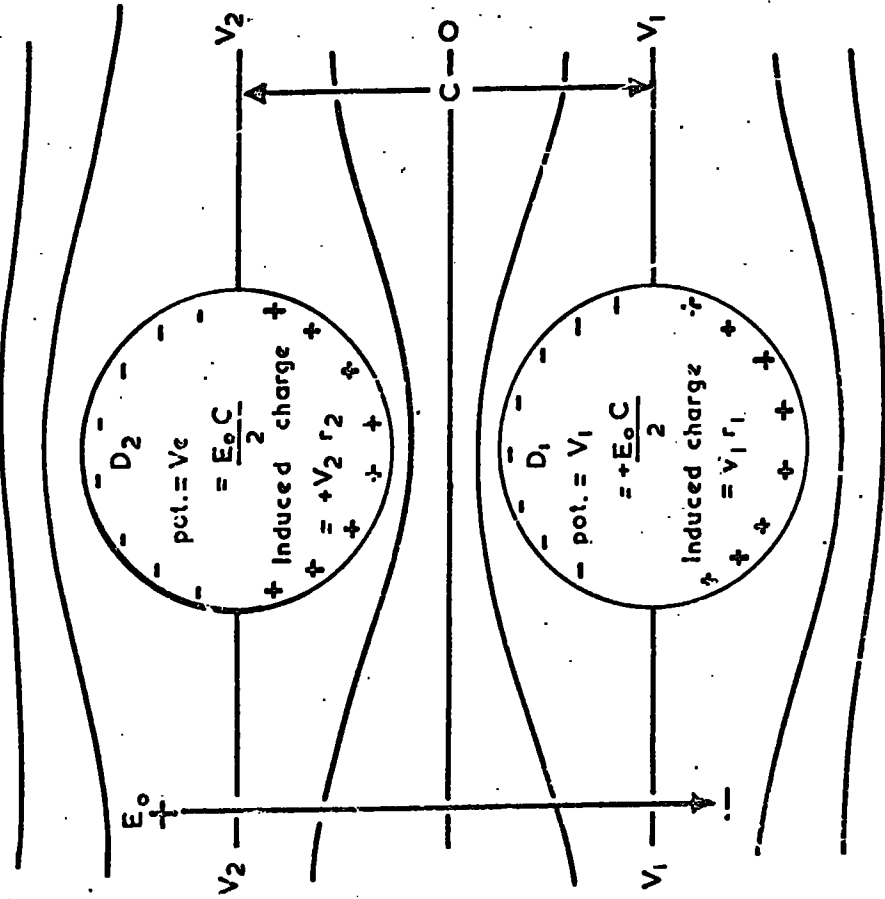


Fig.5.4 (a) Lower curves: average electrostatic charge on precipitation particles at various altitudes; (b) Top curve: corrected temperature as measured with M1313 aircraft psychrometer. (After GUNN).

BEFORE DISCHARGE

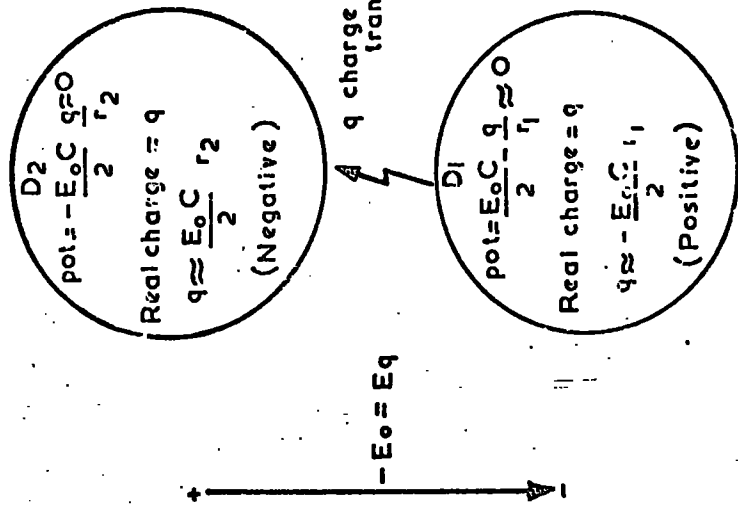


$$r_1 \approx r_2 \approx \frac{C}{2}$$

$$-(V_2 - V_1) = E_0 C$$

(a)

AFTER DISCHARGE



$$r_1 \approx r_2 \approx \frac{C}{2}$$

$$\left(\frac{-E_0 C}{2} + \frac{q}{r_2}\right) - \left(\frac{E_0 C}{2} - \frac{q}{r_1}\right) = 0$$

(b)

Fig.5.5 Transfer of charge. (After SAFTOR).

together so that  $\frac{c}{2} = r_1 = r_2$ . Zero potential is taken half-way between the centres of the drops. When the distance separating the near surfaces of the drops becomes very small, the field between the drops exceeds the critical value for 'break-down', and electrons leave the surface of  $D_1$  and collect on  $D_2$ . Charge will flow until the potential of the drops due to this charge produces a field which is equal in magnitude, but opposite in direction, to that produced by the induced charges. The difference of the potential is

$$(-E_0 c/2 + q/r_2) - (E_0 c/2 - q/r_1) = 0,$$

or

$$-E_0 c^2 = -4q \quad \text{when } r_1 = r_2 = c/2.$$

Now if the drops are separated again, the lower drop leaves with a net positive charge of  $-E_0 c^2/4 = -E_0 r_1^2$ , and the large drop retains a negative charge of  $E_0 c^2/4 = E_0 r_2^2$ . If the drops do not approach on a line parallel to the field, the potential is reduced by a factor of  $\cos\theta$ , where  $\theta$  is the angle between the external field and the line connecting the centres.

The asymmetry of the relative trajectories of two cloud droplets of slightly different sizes is such that a transfer of charge in the opposite direction will not occur, in general, when the smaller drop reaches a position above the centre of the larger drop. Thus, the smaller droplet will receive and retain a positive charge when two freely falling droplets collide under the influence of a negative electrostatic field. This will be the case, with very few exceptions, in the atmosphere. In general, then, one should find both positively and negatively charged droplets in any region of a cloud, but with a tendency for the larger drops to be negatively charged. Because of the difference in falling velocities, positively charged droplets should be more numerous near the top of a cloud, while

negatively charged droplets should predominate in the lower portions. This forced separation of charge areas enhances the atmospheric field and accelerates the charge mechanism. It should be pointed out, however, that two equally large drops can fall to the ground, one immediately after the other, and possess opposite charges of equal magnitude; it is possible that the same two drops, just shortly before, could have been close enough to have become selectively charged.

A large drop will not break up into two equal portions, but into one or two large drops and a number of smaller drops. Just prior to and immediately after actual separation, the more massive portions of a breaking drop generally will be below the smaller portions. Since the separation is mechanical, and therefore comparatively slow, charge transfer will take place immediately after the separation is accomplished. In this instance, due to the negative field of the cloud, the larger drops will acquire a positive charge.

#### 5.5 WEBB and GUNN 1954

Samples of more than 35 natural clouds were passed through a special centrifuge and an ion filter in such a way that the free electricity on the droplets and on the air could be measured separately. The net charge on typical cloud droplets is less than one ion per droplet. This shows either that cloud droplets are not appreciably charged or that both positive and negative droplets are present and the distribution is such as to make the net charge very small. The measurements show that the capture of ions of a preferred sign by cloud droplets is not important.

#### 5.6 BLANCHARD 1955

BLANCHARD's results were obtained for droplets of sea water, newly

formed from bursting bubbles at an air-sea-water interface. Early in his study of breaking bubbles (1953) he found that the droplets produced by a vertical jet were electrically charged. Curve A of Fig.5.6 is for droplets from bubbles which were allowed to break in the presence of an electric field. In this manner all the droplets originating via the jet mechanism obtained, by electrostatic induction, a charge of sign opposite to that of the electrode potential. For a given droplet radius, this charge was substantially the same in the range of fields from  $5 \times 10^3$  to  $3 \times 10^4$  V m<sup>-1</sup>. Curves B, C and D are for the natural charge on the droplets. In these cases the bubbles were allowed to produce droplets before the balancing electric field was applied. It will be noted that the results, unlike those for the induced charges, tend to fall into three separate groupings. The first, for droplets less than 3  $\mu$ m radius, indicates an increase of charge nearly proportional to the fifth power of the radius. The second, for droplets between 3 and 6  $\mu$ m in radius, shows approximately a second-power relationship. The third grouping for droplets greater than 6  $\mu$ m radius, is similar to the second. The maximum charge per unit volume is obtained by droplets of about 3  $\mu$ m radius. At this radius the quantity of charge is nearly identical with that obtained when the bubbles break in the presence of an electric field. He found that the charge on all the drops is positive.

### 5.7 TWOMEY 1956

Measurements made on a mountain summit showed that a high proportion of cloud elements sampled carried appreciable electric charges. Drops in liquid water clouds were consistently positively charged, negative or mixed charges occurring in clouds containing the ice phase. The magnitudes of the positive charges were clearly correlated with diameter Fig.5.7 and 5.8, ranging from around  $10^{-7}$  e.s.u. for droplets 10  $\mu$ m in diameter to above

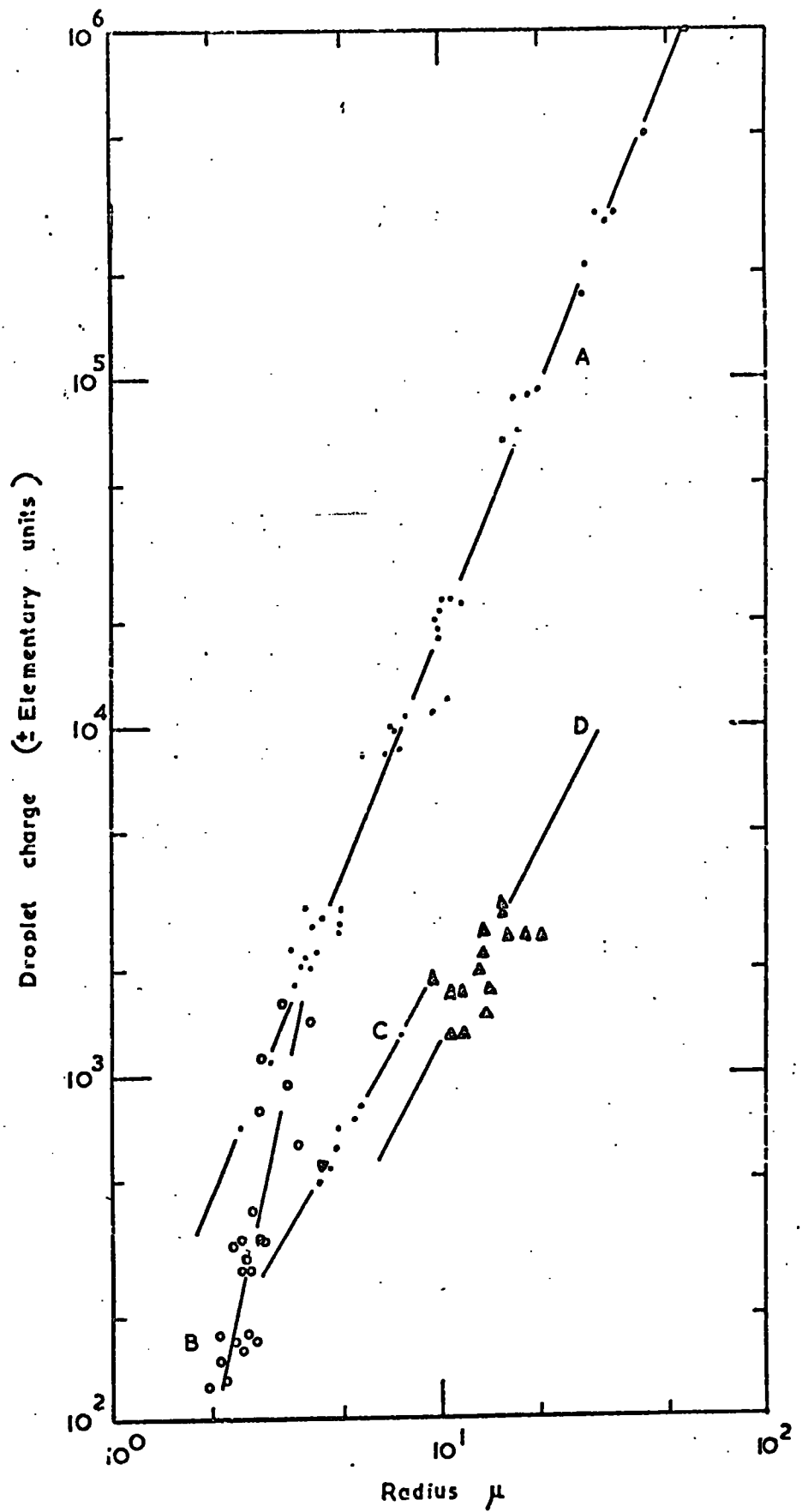


Fig.5.6 Natural and induced charge on droplets from bursting bubbles. (After BLANCHARD).

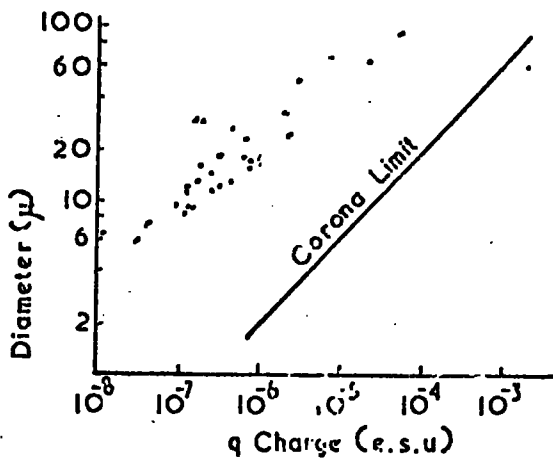


Fig.5.7 Relation of observed charge to droplet diameter (positive charges) - July (1955) results. (After TWOMEY).

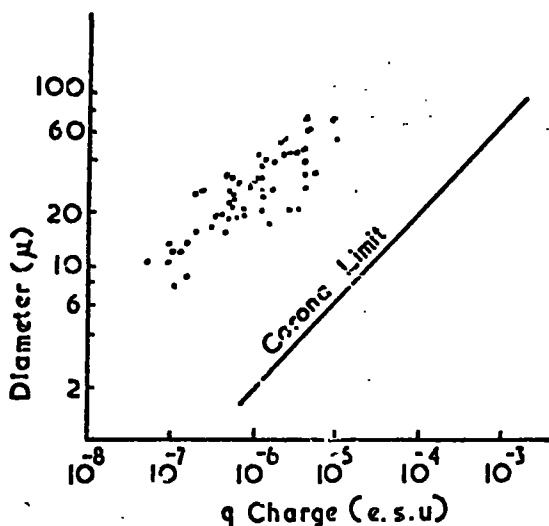


Fig.5.8 Relation of observed charge to droplet diameter (positive charges) - February 1956 results. (After TWOMEY).

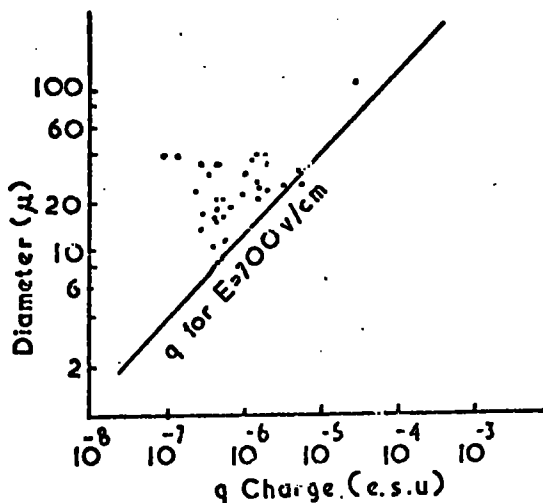


Fig.5.9 Relation of observed charge to droplet diameter (negative charges) - July 1955 results. (After TWOMEY).

$10^{-5}$  e.s.u. for 100  $\mu\text{m}$  droplets. The negative charges were of a similar order of magnitude but were not clearly correlated with droplet diameter Fig.5.9 .

The charges measured should be sufficient to reduce significantly the coalescence rate in the case of cloud elements of the same polarity or to increase it in the case of encounters between elements of opposite polarity. Hence it seems probably that electric charges play an important part in the physics of rain formation. It is suggested that positive charges were accumulated by diffusion of ions into the droplets. It seems necessary to postulate that positive ions are preferentially absorbed, possibly as a result of the arrangement of molecules in the liquid surface layer. The production of negatively charged cloud elements is attributed to a process of the kind described by LUEDER (1951), in which the collection of super-cooled water resulted in the collecting body acquiring a negative charge.

#### 5.8. PHILLIPS and KINZER 1957

The size and the free electric charge of more than 6000 individual natural cloud droplets were measured. The measurements were made at a mountain laboratory in the S.E. United States in stratocumulus clouds and in thunderstorm-associated clouds. Stratocumulus cloud with fair-weather electric fields were found to have approximately Gaussian charge-distributions symmetrical about zero charge. The magnitude and distribution of charges observed on these non-stormy clouds approach values described recently by R. GUNN (1955) in his theory of aerosol electrification by the diffusion of environmental light ions. Thundercloud droplets were highly electrified and within given cloud volumes the droplets were charged entirely positive, entirely negative, or fractionally positive and negative.

5.9 ALLEE and PHILLIPS 1958

Four different clouds were investigated during the winter season of 1957-58. For each cloud, the average droplet radius,  $\bar{a}$ , was calculated by

$$\bar{a} = \frac{1}{n} \sum_{i=1}^h n_i a_i,$$

where  $n$  is the total number of drops in the distribution,  $n_i$  is the total number of cloud droplets in the  $i$ th interval with the radius  $a_i$ , and  $h$  is the number of cloud droplet radius intervals. This average radius was substituted for the effective radius in the equation (5.2) developed by GUNN (1955)

$$F_x = \frac{F_t e}{(2\pi aKT)^{1/2}} \exp \left\{ \frac{-(x - \frac{aKT}{e^2} \ln \frac{\lambda_+}{\lambda_-})^2}{\frac{2aKT}{e^2}} \right\}$$

A percentage plot of  $\frac{F_x}{F_t}$  versus  $x$  from equation (5.2) gives the theoretical equilibrium distribution of charge on a cloud droplet aerosol.

The average observed magnitude of charge per droplet,  $\bar{q}$  is calculated from the distribution data by the relationship

$$\bar{q} = \frac{1}{n} \sum_{i=1}^h n_i |q_i|, \quad (5.4)$$

where  $n$  is the total number of droplets in the distribution,  $n_i$  is the total number of cloud droplets in the  $i$ th interval with the charge magnitude  $|q_i|$ , and  $h$  is the number of cloud-droplet-charge intervals. From equation (5.2) the average magnitude of the theoretical charge is

$$\bar{q} = \left( \frac{2aKT}{\pi} \right)^{1/2} \quad (5.5)$$

A comparison of the average values obtained from equations (5.4) and (5.5) where again the effective droplet radius  $a$  is defined by equation (5.2) becomes an excellent measure of how nearly the theoretical equilibrium charge

distribution is approximated by the charge distributions within natural clouds.

Fig.5.10 is a summary of the droplet charge versus droplet radius from sources as noted.

#### 5.10 SHISHKIN 1963

He suggested a charging mechanism for coalescence rain based on FRENKEL's (1944) ideas. He assumed a constant potential for all cloud droplets of  $-10^{-4}$  e.s.u. and calculated the resulting charge after coalescence. He also calculated the electric field inside the cloud by assuming a constant supply of small charged droplets. For a rain current of 10 mm per hr the electric field reaches breakdown conditions inside the cloud. SHISHKIN states that this model gives thunerstorm conditions. Unexplained, however are his assumptions for the charging of small droplets, the influence of the opposite polarity of charges that must stay somewhere in the cloud, and the influence of conduction and corona currents in such very high fields.

#### 5.11 AZAD and LATHAM 1969

They studied the electrohydrodynamics of a process which may be responsible for the electrification of warm clouds. If two charged drops are separated in an electric field of strength  $E$  the mutual interaction of the polarization and applied charged on the drops results in a field in their near surfaces which is different from and generally greater than that in the surface of an isolated drop. The value of  $E$  required to effect disintegration will therefore decrease rapidly as the separation of the drops is reduced. TAYLOR's spheroidal assumption and DAVIS's (1964) calculations of the enhancement of the field between a pair of spherical conductors have been employed in calculations of the field required to disintegrate one of a pair of drops

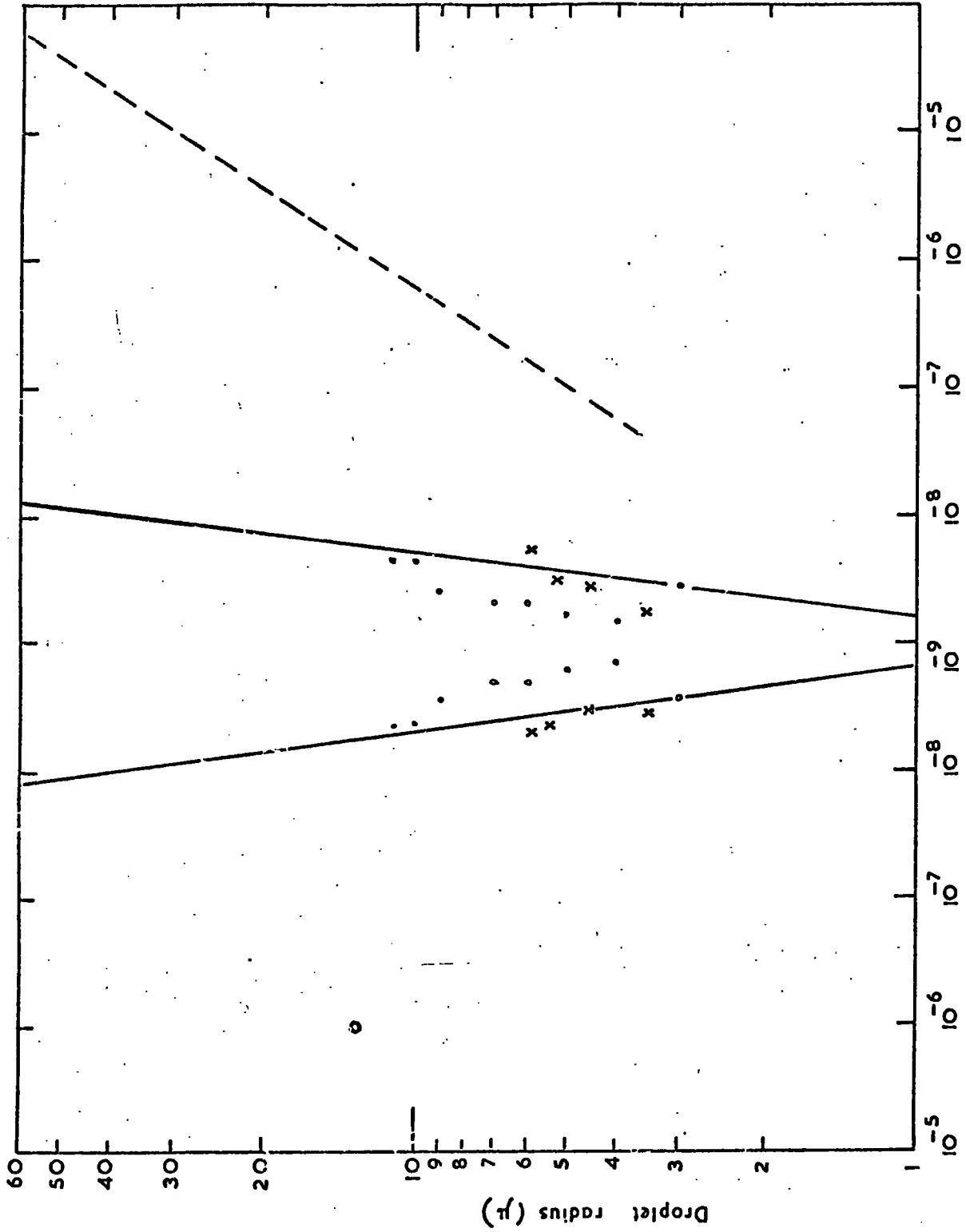


Fig.5.10 Positive and negative average cloud-droplet charge versus radius for supercooled droplets (ALLEE and PHILLIPS), warm droplets (PHILLIPS and KINZER, 1958), near-freezing droplets (TWOMEY, 1956), theoretical average charge (GUNN, 1955); x Averages of 305 droplets, ALLEE and PHILLIPS; . Averages of 4319 droplets PHILLIPS and KINZER (1958); --- Regression curve for 30 positive droplets TWOMEY (1956); o Theoretical average charge GUNN (1955).

of radii  $R_1$  and  $R_2$  carrying charges  $Q_1$  and  $Q_2$ , whose line of centres is inclined at an angle  $\phi$  with the vertical electric field. The polar and equatorial equilibrium conditions provided a quartic equation which could be solved numerically to find critical values of  $E (R_2/T)^{1/2}$  for various values of radii, charges and drop separation. The predicated values of  $E (R_2/T)^{1/2}$  required to effect disintegration agreed well with experimental values determined from photographs by SARTOR and ABBOTT (1968) showing the separation at which a liquid bridge was formed between the near surfaces of a pair of charged drops falling in an electric field. Additional support for the accuracy of the computed disintegration criteria was provided by measurements made with pairs of drops suspended from mechanical supports. Theory and experiment agreed quite closely over a wide range of values of  $R_1$ ,  $R_2$ ,  $Q_1$ ,  $Q_2$ ,  $\phi$  and drop separation.

#### 5.12 LATHAM and SMITH 1969

An instrument has been devised which will measure continuously the charge and dimensions of individual ice crystals or water droplets within clouds at ground level. If its collection efficiency for cloud particles were established it could then also be used to determine particle-size distributions and volume charge densities inside clouds.

A collimated beam of particles passes through a transverse electric field before impinging on a moving belt of 35-mm film coated with Formvar which has been softened immediately prior to exposure to the beam. Each particle is deflected by an amount proportional to its charge-to-mass ratio. The dimensions, type and charge of each collected particle can therefore be determined by subsequent analysis of the replicas using a stop-motion projector allied to a data recording system. If required, the dimensions of selected particles can be determined more precisely using an electron

scanning microscope. The minimum detectable charge on a droplet of radius  $r$  cm and terminal velocity  $V$  cm s<sup>-1</sup> is given approximately by

$$q_{\min.} \approx 5 \times 10^{-2} r^3 V^2 \text{ e.s.u.}$$

### 5.13. COLGATE and ROMERO 1970

Cloud drop charge and size have been measured with tethered balloon-borne equipment in the lower few hundred meters and at an early stage of a forming thunderstorm by photographing the droplets in a combined sound wave and electrostatic field. The drop size distribution shows a peak at 7 to 8  $\mu\text{m}$  in diameter, and the charge distribution at each of several drop sizes shows an average negative charge of  $-18 \times 10^{-8}$  e.s.u., and a mean absolute charge  $\langle |q| \rangle = K_0 r^2$ , where  $K_0 = 1.72 \times 10^4$  e.s.u. m<sup>-2</sup>. At an observed average of  $2 \times 10^8$  to  $3 \times 10^8$  drops m<sup>-3</sup>, this corresponds to a space charge concentration of about  $-50$  e.s.u. m<sup>-3</sup> or  $10^{11}$  elementary charges m<sup>-3</sup> Fig. 5.11 .

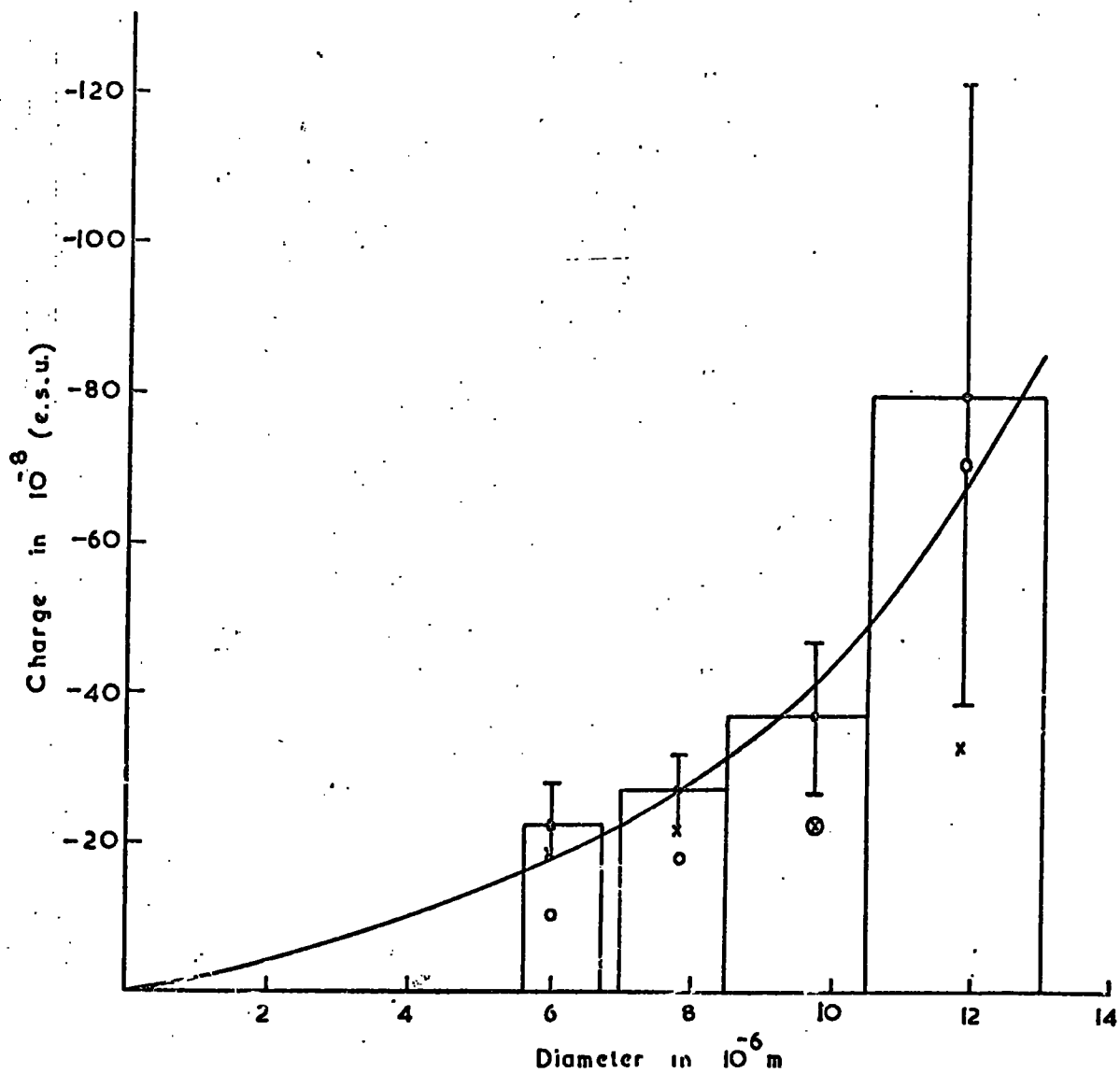


Fig.5.11 The negative of the mean of the absolute charge (solid circles) as a function of radius. The error bars centered on the dots are only an approximation to the error. The ordinate is negative to show the average charge (open circles). In addition, the negative of the median of the absolute charge is shown by crosses. The solid curve is drawn such that  $\langle |q| \rangle = K_0 r^3$  with  $K_0 = 1.72 \text{ esu cm}^{-2}$ . (After COLGATE and ROMERO).

## CHAPTER 6

### A LABORATORY EXPERIMENT

#### 6.1 The diffusion chamber

The diagram shown in Fig.6.1 illustrates the important features of the chamber used for producing nucleus-free air and subsequently studying specific types of nuclei.

The lower cold plate is maintained by the use of crushed ice with water in a hollow box of brass of dimensions  $0.2\text{ m} \times 0.2\text{ m} \times 0.2\text{ m}$ . The cold plate of the cloud chamber rests on the top of this box. Resting on the cold plate is a perspex box of dimensions  $0.2\text{ m} \times 0.2\text{ m} \times 0.1\text{ m}$ . The chamber has two windows suitably placed, at right angles to each other, for viewing and lighting purposes. On top of this is a flat plate of brass, warmed with a soldering iron 25-watt heater, in contact with the under surface of the warm plate a small pad of felt soaked with water serves as source of vapour in the chamber. The diameter of this pad is less than half of the diameter of the inside of the chamber; otherwise, a large amount of condensed water will form on the sides of the chamber and limit visibility.

Ordinary air containing nuclei was allowed to enter the chamber, through a glass tube 10 mm in diameter, which is normally kept closed. The temperature gradient inside the chamber was measured by horizontal copper-constantan thermo-couples. Three thermo-couples were employed in the chamber and were attached to the top, middle and the bottom of the chamber. All the couples were constructed identically, having the same length and thus the same resistance. The complete circuit of the thermo-couples is shown in Fig.6.2.

A scalamp galvanometer was used to indicate the e.m.f. produced, and the resistance R was adjusted during the calibration so that for temperatures

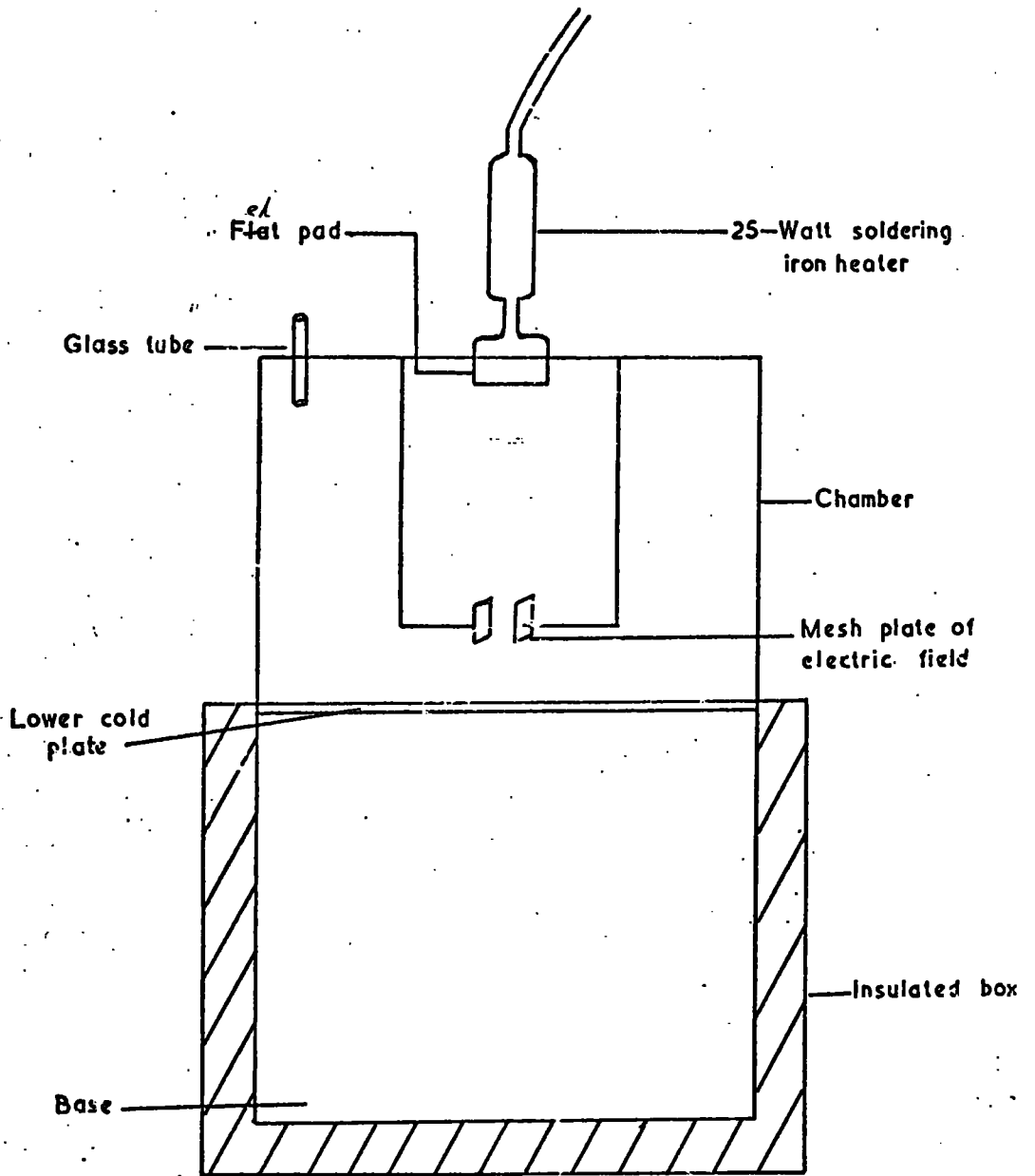


Fig.6.1 Diffusion Chamber.

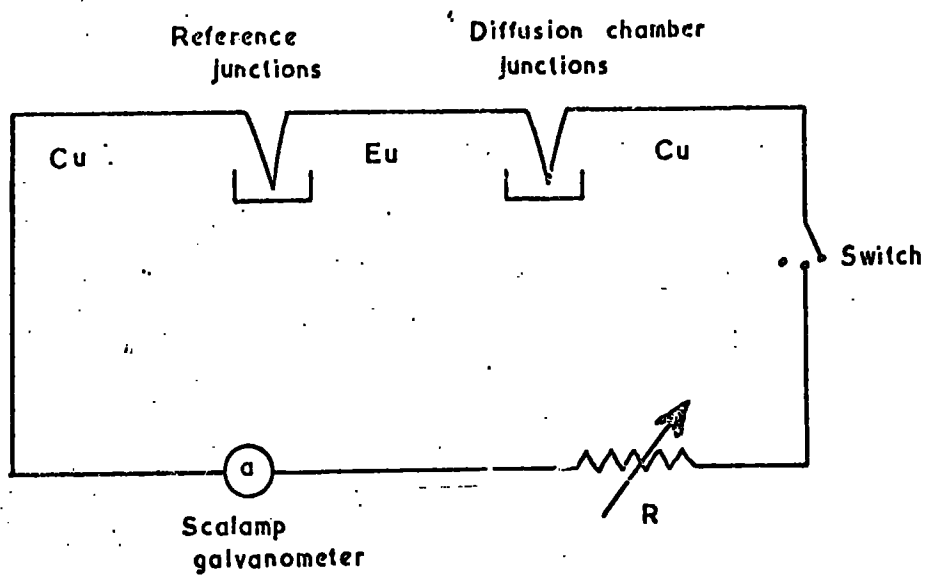


Fig.6.2 Thermo-Couple circuit.

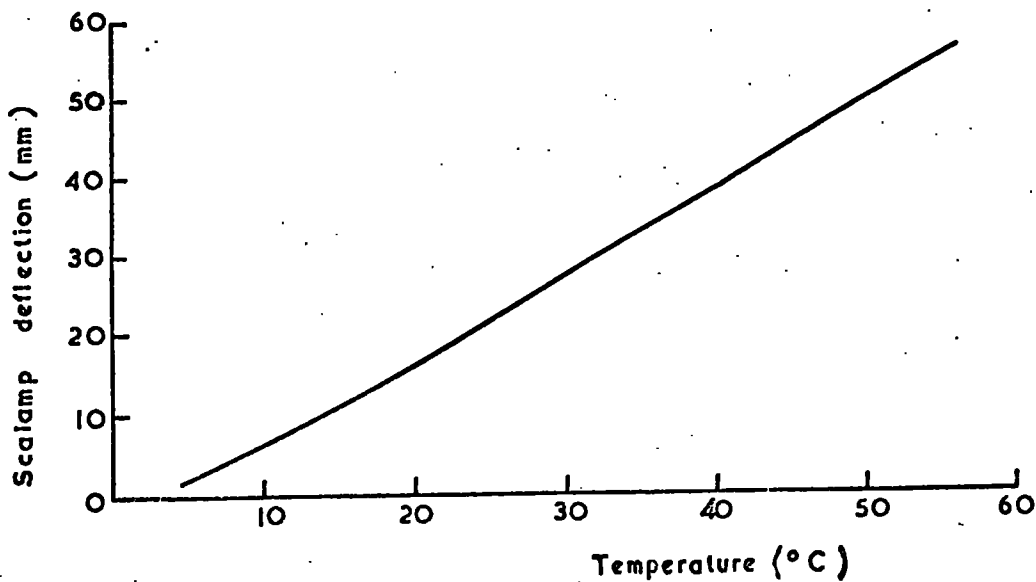


Fig.6.3 Calibration curve of the thermo-couples.

between 40°C to 0°C a deflection of about 1mm on the scalamp was equivalent to 1°C temperature difference Fig.6.3 , this being the range over which the series of experiments was to be performed. The switch was used to select the individual thermo-couples in turn.

The droplets were observed visually through a low-power binocular microscope. The light source used for viewing is a high intensity type giving a parallel beam. The work must be done in a darkened room.

An electric field was applied inside the chamber by two parallel plates of dimensions 20 mm × 20 mm; each plate was attached to a rod, covered with plastic insulating sleeving, which passed through a hole in the top plate of the chamber. The circuit for the electric field is shown in Fig.6.4 . A d.c. power supply unit was used for a proper value of the voltage, and a series resistance of 1 MΩ protected the system from excess current in the event of an accidental short circuit.

The chamber was well insulated with expanded polystyrene and fibreglass, to reduce the convection. A small box filled with water was put in the light path to absorb the heat.

## 6.2 Operation of the chamber

The chamber was operated as follows:-

The felt pad was saturated with water and then heated by bringing a soldering iron into contact with the top of the chamber until the chamber reached operating temperature. While the vapour flow was being established; the base was being cooled. Whilst the droplets were building up, the optical system was adjusted. The cloud of droplets formed just above the base of the chamber.

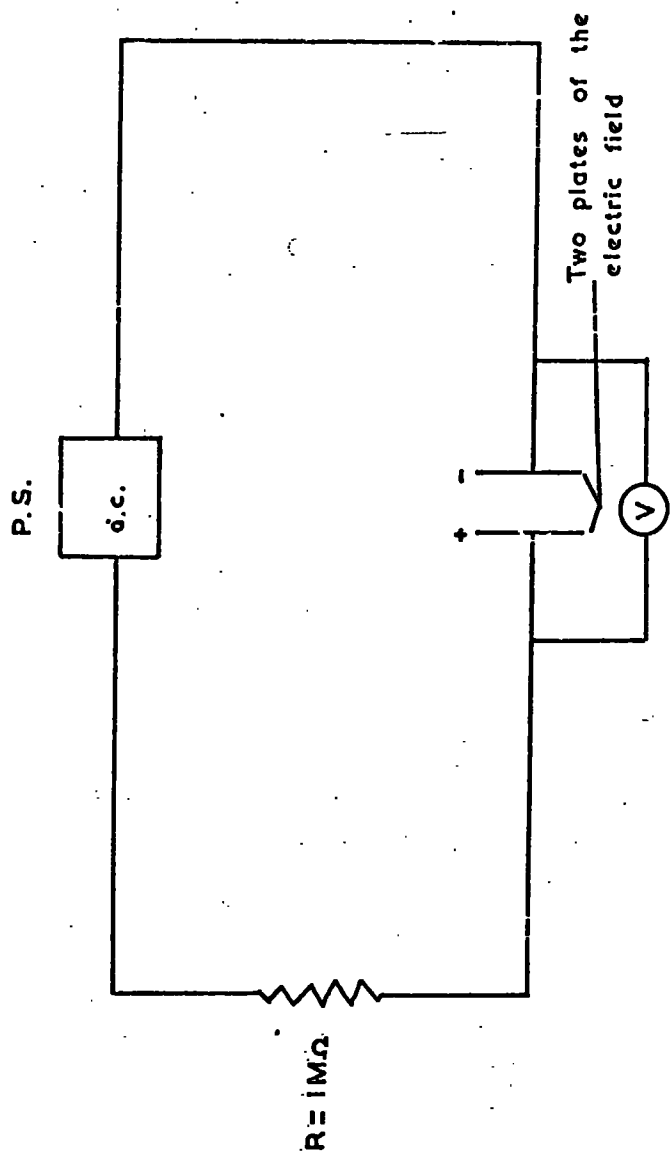


Fig.6.4 Electric field circuit.

### 6.3 Measurement of charges

In this experiment the droplets generated in the chamber were allowed to fall between a pair parallel plates where they subject to a horizontal electric field 30 and 80 KV m<sup>-1</sup>. The deflection of the droplet Fig.6.5 in a given time was measured directly by reading the microscope scale. From this deflection, the horizontal and vertical velocity components of the droplet can be calculated.

A photographic technique has been tried to calculate the charge on the droplet. The aim was to photograph the droplet deflection in the field by fitting a camera to the eyepiece of the microscope. Unfortunately it was not possible to obtain satisfactory photographs of the droplets in the chamber in spite of using a high speed film to match the particle speed and varying the illumination inside the chamber.

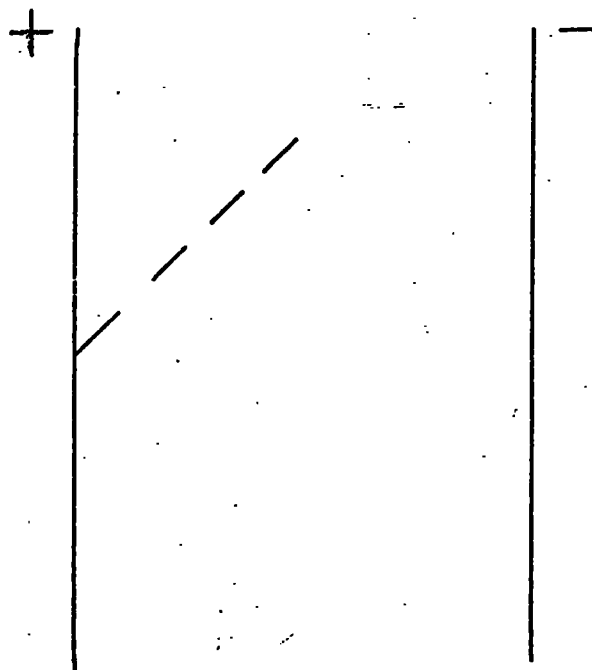


Fig.6.5 The deflection of the droplet inside the field.

C H A P T E R 7

THE OBSERVED CHARGES ON THE DROPLET

7.1 Results and data analysis

The most important characteristic of suspensions of small particles in air is that they are not in equilibrium. The particles are continually diffusing to the surrounding walls, and colliding with each other and coalescing. The motion of the particles is restricted by the viscosity of the air. For spheres of radius  $a$ , falling with velocity  $v_1$ , the viscous force is given by Stokes's law,

$$F = 6\pi \eta a v_1$$

where  $\eta$  is the viscosity of the medium.

For steady fall, this force is equal to the weight of the particle,

$$\text{i.e.} \quad 6\pi \eta a v_1 = \frac{4}{3} \pi a^3 \rho g$$

$$\text{and} \quad a = \left( \frac{g}{2} \frac{\eta v_1}{\rho g} \right)^{1/2}$$

where  $\rho$  is the density of the particle ( $\text{kgm}^{-3}$ ), and  $g$  is the acceleration due to gravity ( $\text{ms}^{-2}$ ). Hence taking for the viscosity of air  $\eta = 1.81 \times 10^{-5} \text{ kgm}^{-1}\text{s}^{-1}$ , the radius of a sphere falling steadily under gravity is given by

$$a = A v_1^{1/2} \tag{7.1}$$

where

$$\begin{aligned} A &= \left( \frac{g}{2} \frac{\eta}{\rho g} \right)^{1/2} \\ &= 10^{-4} \text{ ms} \end{aligned}$$

Similarly the motion of the droplet in a horizontal electric field will be given by

$$qE = 6\pi \eta a v_2$$

where  $q$  is the charge of the droplet (C), and  $E$  is the electric field ( $V m^{-1}$ ),  $v_2$  is the velocity of the droplet inside the field ( $ms^{-1}$ ). From the above equation we find that

$$\begin{aligned} q &= 6\pi \eta a \frac{v_2}{E} \\ &= B \frac{a v_2}{E} \end{aligned} \quad (7.2)$$

where

$$\begin{aligned} B &= 6\pi\eta \\ &= 34.4 \times 10^{-5} \text{ kgm}^{-1}\text{s}^{-1} \end{aligned}$$

The charge of the droplet was calculated by using equations (7.1) and (7.2). The measurements were made with two values of the electric field,  $300kV m^{-1}$  and  $600kV m^{-1}$ . In both cases the charge and the radius of the droplet were calculated. The average charges on the droplet in both cases were about  $5e$  which indicates that the charge on the droplet is not affected by the field. The average charge found in this experiment is about the same as that reported by GUNN (1955). The radii of the droplets seen in my experiment, regardless of their sign, were between 1 and 2  $\mu m$ . The percentage of larger droplets was small. Fig.7.1 summarizes the percentage of droplets seen as a function of their radius. Fig.7.2 gives the percentage of the droplets as a function of their charges. Again here drops with charges exceeding  $10e$  are rare. The distribution of charges among the droplets is shown in Fig.7.3. It may indicate that the distribution is a Gaussian as predicted

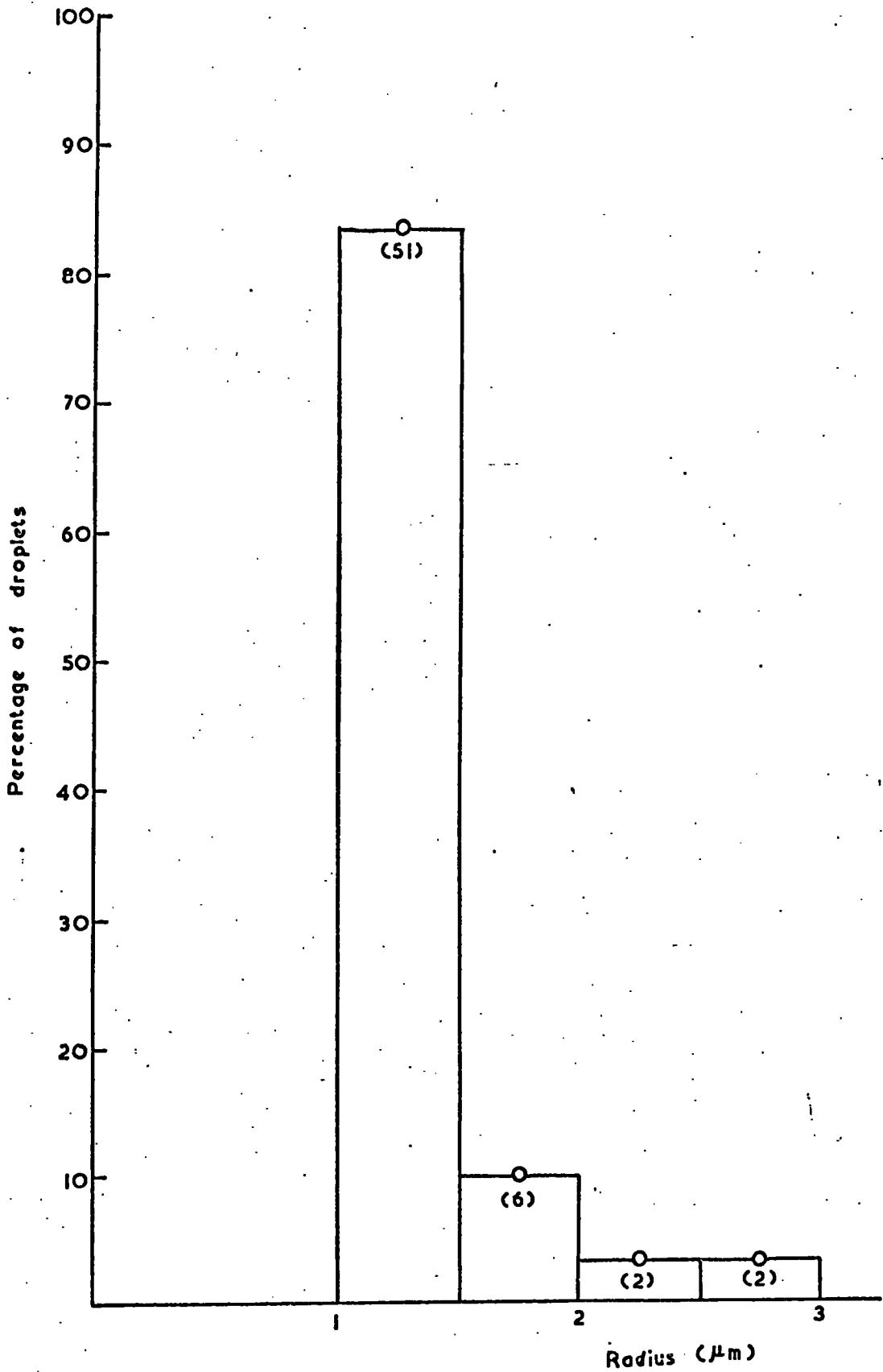


Fig.7.1 The percentage of the droplets seen as a function of their radius. The figures between the brackets represent the number of the droplets seen.

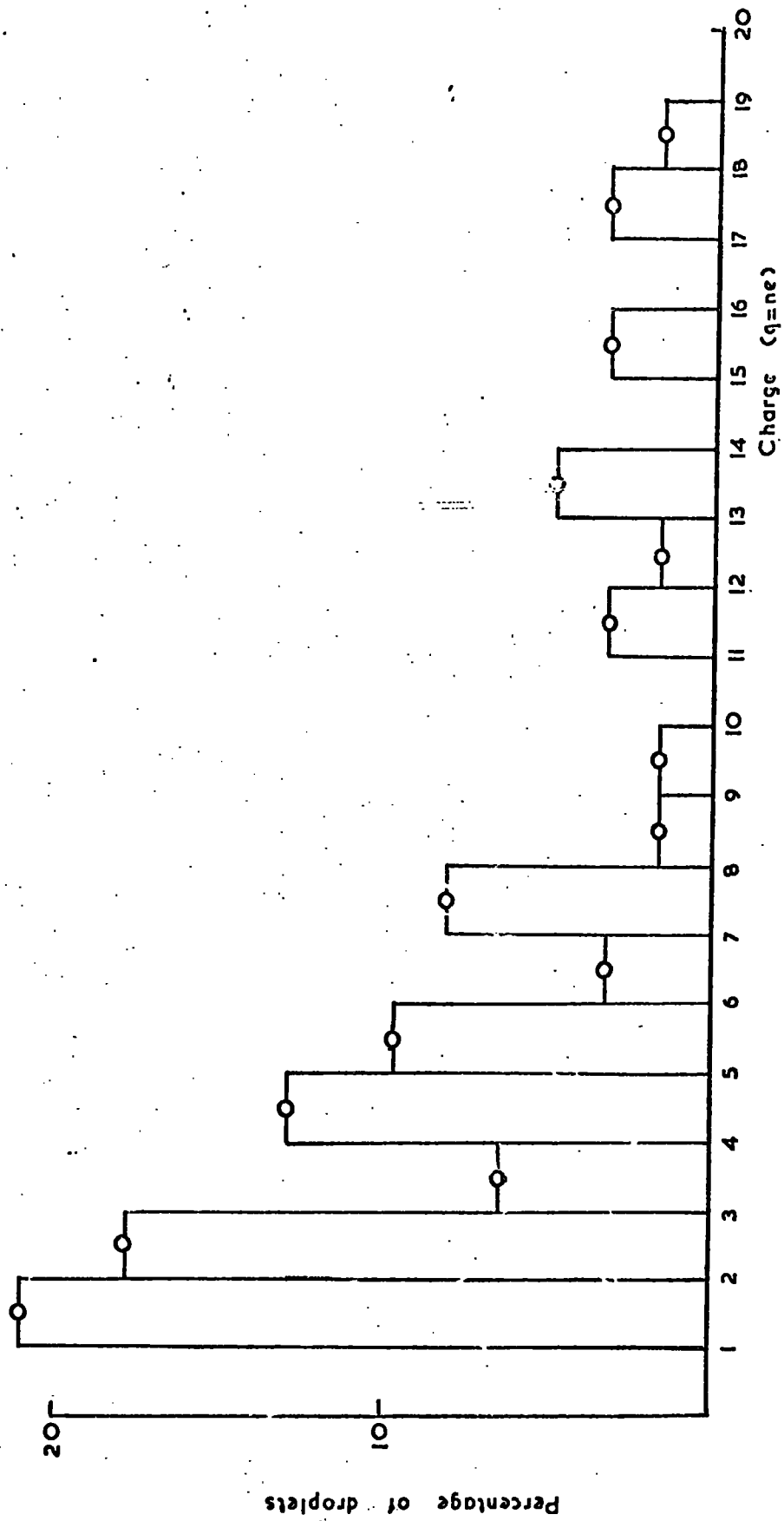


Fig. 7.2 Percentage of the droplets seen as a function of their charges

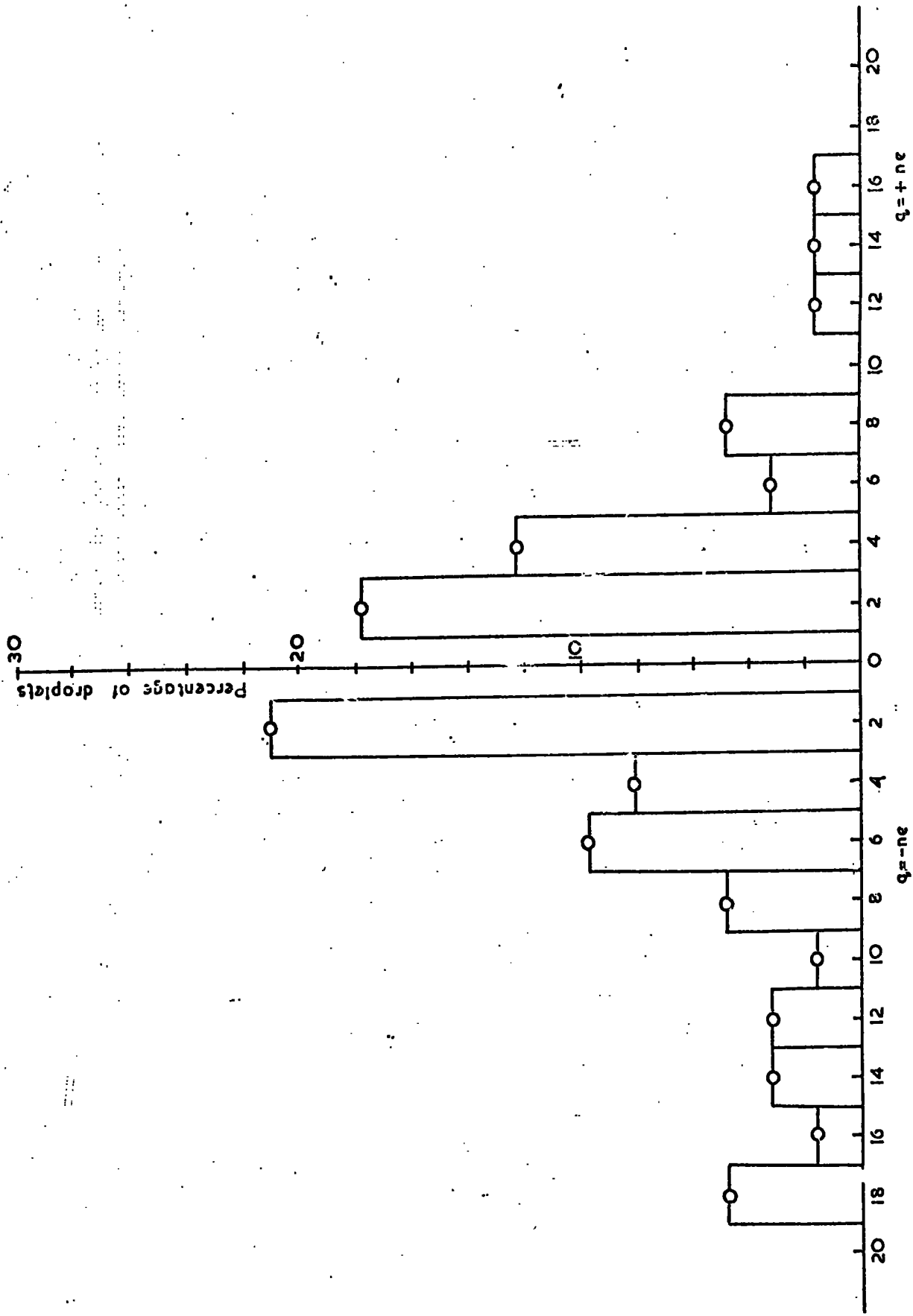


Fig.7.3 The distribution of charges among the droplets.

by GUNN (1955). The charge of the droplets as a function of their radius is shown in Fig.7.4.

## 7.2 Suggestions for further work

The method used in this work to deduce the charge on the droplets is not very accurate as the charges could be estimated only to about  $\pm 10\%$ . The error in measuring the charge on the droplets was caused by the difficulty of making instantaneous measurements of time and deflection.

The photographic method is an alternative which could be used to estimate the charge on droplets with greater accuracy. From measuring the track length on the photograph and by knowing the exposure time of the camera, one could calculate the velocity of the droplet. To obtain good photographs the kind of film, illumination inside the chamber and the magnification of the microscope must be carefully regulated. The exposure time is determined by the velocity of the droplets. The shutter speed must be such that the track length is long enough to be measured accurately. The resolution of the film and the illumination must be such that small droplets can be seen.

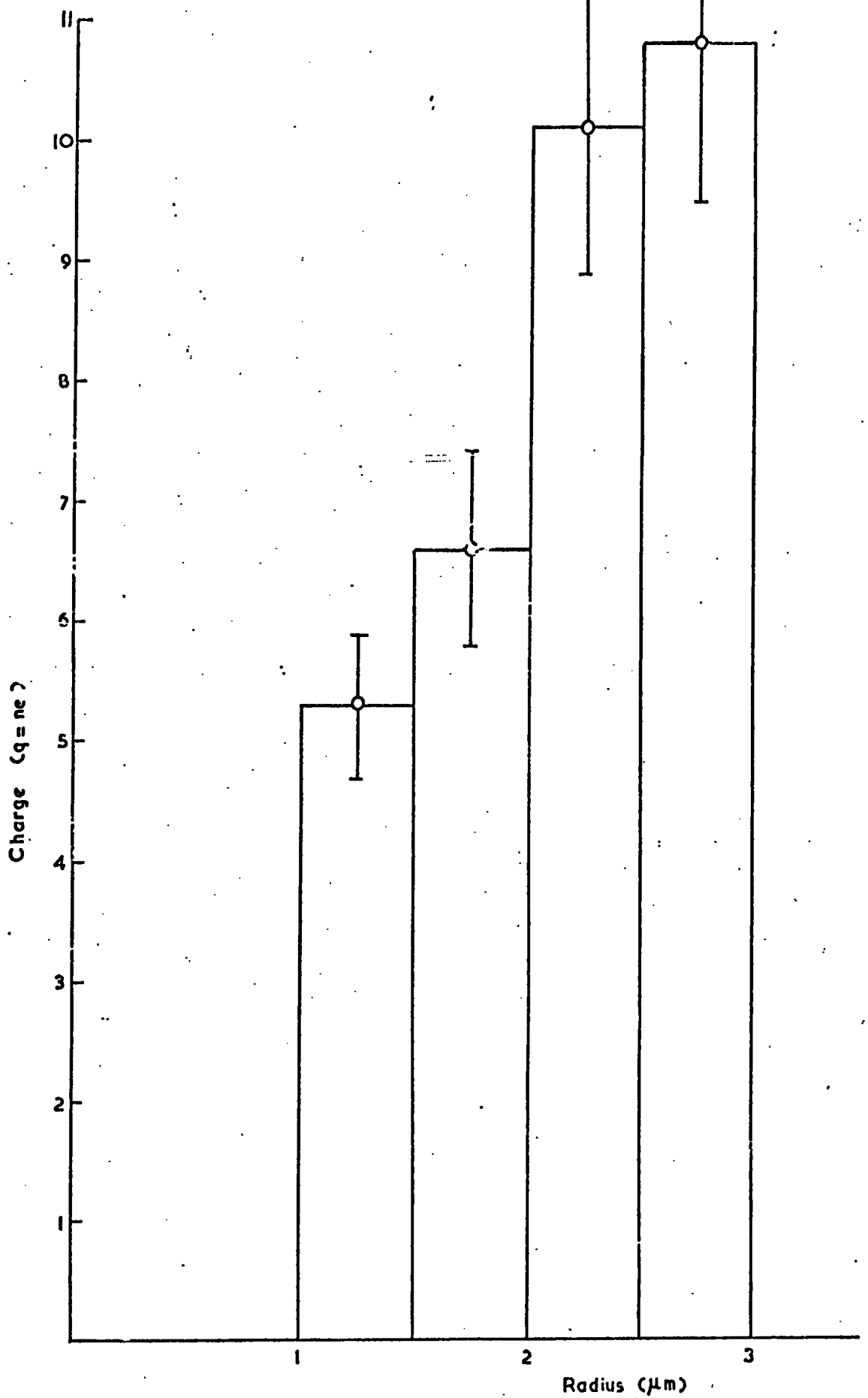


Fig.7.4 The charge on the droplets as a function of their radius. The error bars represents an error of 10%.

ACKNOWLEDGEMENTS

The author would like to express to Dr. W. C. A. Hutchinson her sincere appreciation of suggestion of the project, supervision and constant advice, and to Professor G. D. Rochester, Head of the Physics Department, her thanks for providing facilities.

The author is indebted to all members of the Atmospheric Physics Group for their advice, and in particular to Mr. Jack Moralee for construction of the apparatus. Mrs. S. M. Robson is thanked for the speed and efficiency with which she typed this thesis. Thanks are also due to Miss P. A. Wallace for drawing the diagrams.

References

- ALLEE, A. P. and PHILLIPS, B. B. (1959) Measurements of cloud-droplet charge, electric field, and polar conductivities in supercooled clouds  
J. Met. 16, 405-10.
- AZAD, K. A. and LATHAM, J. (1970) The disintegration of charged drop-pairs in an electric field  
J. Atmos. Terr. Phys. 32, 345-54.
- APPLETON, E. V., WATSON-WATT, R. A. and HERD, J. F. (1926) On the nature of atmospheric III.  
Proc. Roy. Soc. A, 111, 654-77.
- ARNDT, P. and KALLMANN, H. (1925) Über den Mechanismus der Aufladung von Nebelteilchen  
Z. Physik, 35, 421-41.
- BARNARD, V. (1951) The approximate mean height of the thundercloud charges taking part in a flash to ground  
J. Geophys. Res. 56, 33-5.
- BERGERON, T. (1933) On the physics of cloud and precipitation  
Gen. Ass. Int. Un. Geod. (Lisbon) pp.156-70.
- BLANCHARD, C. D. (1955) Electrified droplets from the bursting of bubbles at an air-sea water interface  
Nature 175, 334-6.
- BYERS, H. R. (1965) 'Elements of cloud physics'  
The University of Chicago Press, Chicago and London.
- CHALMERS, J. A. (1956) The vertical electric current during continuous rain and snow  
J. Atmos. Terr. Phys. 9, 311-21.
- CHALMERS, J. A. (1957) 'Atmospheric Electricity'  
First edition, Pergamon Press.
- CHALMERS, J. A. (1959) The electricity of nimbostratus clouds  
Recent Advances in Atmospheric Electricity, Pergamon Press
- COLGATE, A. S. and JOHN, M. R. (1970) Charge versus drop size in an electrified cloud  
J. Geophys. Res., 75, 5873-80.
- DAVIS, M. H. (1964) Quart. J. Mech. Appl. Math. 7, 499.
- EAST, T. W. R. and MARSHALL, J. S. (1954) Turbulence in clouds as a factor in precipitation  
Quart. J. R. Met. Soc. 80, 26.

- FLETCHER, N. H. (1962) 'The physics of rain clouds'  
Cambridge University Press.
- FRENKEL, Y. I. (1944) A theory of the fundamental phenomena of  
atmospheric electricity  
J. Phys., Moscow, 8, 285-304.
- FRENKEL, J. (1946) Influence of water drops on the ionizat-  
ion and electrification of air  
J. Phys., U.S.S.R., 10, 151-8.
- FRENKEL, J. (1947) Atmospheric electricity and lightning  
J. Franklin Inst., 243, 287.
- FRANKLIN, B. (1752) Phil. Trans. Roy. Soc. 47, 289.
- GEORGE, D. J. (1971) Mother of pearl clouds  
Weather, pp.7.
- GISH, O. H. and (1936) Electrical conductivity of air to an alti-  
SHERMAN, K. L. tude of 22 km  
Nat. Geogr. Soc. Contrib. Tech. papers,  
Stratosphere Ser., No.2, pp.94.
- GISH, O. H. and (1950) Thunderstorms and the earth's general  
WATT, G. R. electrification  
J. Geophys. Res. 55, 473-84.
- GUNN, R. (1948) Electric field intensity inside of natur-  
al clouds  
J. Appl. Phys. 19, 481-4.
- GUNN, R. (1952) The electrification of cloud droplets in  
non-precipitating cumuli  
J. Met. 9, 397-402.
- GUNN, R. (1954) Diffusion charging of atmospheric drop-  
lets by ions, and the resulting combin-  
ation coefficients  
11, No.5, 339-47.
- GUNN, R. (1955) The statistical electrification of aero-  
sols by ionic diffusion  
J. Colloid Science, 10, 107-19.
- GUNN, R. (1955) Droplet electrification processes and  
coagulation in stable and unstable clouds  
J. Met. 12, No.6, 511-18.
- GUNN, R. (1957) The non-equilibrium electrification of  
raindrops by the association of charged  
cloud droplets  
J. Met. 14, No.4, 326-31.
- JUNGE, C. E. (1958) In advances in Geophysics, ed. H. LANDS-  
BERG and J. VAN MIEGHEM (New York:  
Academic Press) 4, 1.

- KUETTNER, J. (1950) The electrical and meteorological conditions inside thunderclouds  
J. Met. 7, 322-31.
- LANGMUIR, I. (1944) Supercooled water droplets in rising currents of cold saturated air  
G. E. Res. Lab. Rep. W-33-106-Sc-65.
- LATHAM, J. and SMITH, M. H. A ground-based instruments for the continuous measurement of charge on cloud particles  
Quart. J. R. Met. Soc. 96, 408.
- MALAN, D. J. and SCHONLAND, B. F. J. (1951) The distribution of electricity in thunderclouds  
Proc. Roy. Soc. A, 209, 158-77.
- MASON, B. J. (1957) 'The Physics of Clouds'  
University Press, Oxford.
- MAGONO, C. and ORIKASA, K. (1960) J. Met. Soc. Japan II, 38, No.4.
- MAGONO, C. and ORIKASA, K. (1961) J. Met. Soc. Japan II, 39, No.1.
- MALAN, D. J. (1963) 'Physics of lightning'  
The English University Press LTD.
- MILLIKAN, R. A. (1911) The isolation of an ion, a precision measurement of its charge, and the correction of Stokes's law  
Phys. Rev. 32, 349-77.
- PATON, J. (1955) Quart. J. R. Met. Soc. 81, 107.
- PAUTHENIER, M. and LOUFOULLAH, N. (1950) Le Balayage électrique des brouillards  
C. R. Acad. Sci. Paris, 231, 953.
- PETTERSEN, S. (1958) 'Introduction to Meteorology' 2nd edition,  
McGRAW-HILL BOOK COMPANY, INC.
- PHILLIPS, B. B. and KINZER, D. G. (1958) Measurements of the size and electrification of droplets in cumuliform clouds  
J. Met. 15, 369-74.
- PIERCE, E. T. (1955) Electrostatic field changes due to lightning discharges  
Quart. J. R. Met. Soc. 81, 211-28.
- CHALMERS, J. A. and RAMSAY, M. W. (1960) Measurements of the electricity of precipitation  
Quart. J. R. Met. Soc. 86, 530-9.
- REYNOLDS, S. E. and NEILL (1955) The distribution and discharge of thunderstorm charge centre  
J. Met. 12, 1-12.

- SARTOR, D. (1953) A laboratory investigation of collision efficiencies, coalescence and electrical charging of simulated cloud droplets  
J. Met. 11, 98-103.
- SARTOR, D. and ABBOTT, C. E. (1968) J. Geophys. Res. 73, 6415.
- SAFFMAN, P. G. and TURNER, J. S. (1956) On the collision of drops in turbulent clouds  
J. Fluid Mech. 1, 16.
- SCHONLAND, B. F. J. (1928) The polarity of thunderclouds  
Proc. Roy. Soc. A, 118, 233-51.
- SCHONLAND, B. F. J. (1953) 'Atmospheric Electricity' 2nd edition, London: METHUEN and CO. LTD., New York: JOHN WILEY and SONS, INC.
- SCORER, R. S. (1964) Mother of pearl clouds  
Weather, No.4, 115.
- SHISHKIN, N. S. (1963) The role of the coagulation of charged cloud particles in the development of thunderstorm phenomena  
Prob. of Atm. and Space Elec. Montreux Conf., 268-79.
- SIMPSON, G. C. (1949) Atmospheric electricity during disturbed weather  
Geophys. Mem. Lond. 84, 1-15.
- SIMPSON, G. C. and ROBINSON, G. D. (1940) The distribution of electricity in thunderclouds II  
Proc. Roy. Soc. A, 177, 281-329.
- SIMPSON, G. C. and SCARSE, F. J. (1937) The distribution of electricity in thunderclouds  
Proc. Roy. Soc. A, 161, 309-52.
- SMITH, L. G. (1954) Electric field meter with extended range  
Rev. Sci. Instrum. 25, 510-13.
- SMITH, L. G. (1955) The electric charge on raindrops  
Quart. J. R. Met. Soc. 81, 23-47.
- STRINGFELLOW, F. M. (1969) Ph.D. Thesis, Durham University.
- TAYLOR, G. I. (1964) Proc. Roy. Soc. A, 280, 383.
- TWOMEY, S. (1956) The electrification of individual cloud droplets  
Tellus. 8, 445-52.
- WEBB, L. W. and GUNN, R. (1955) The net electrification of natural cloud droplets at the earth's surface  
J. Met. 12, 211-14.

- WHIPPLE, F. J. W. (1929) On the association of the variation of electric potential gradient in fine weather with the distribution of thunderstorms over the globe  
Quart. J. Roy. Met. Soc. 55, 1.
- WILSON, C. T. R. (1922) The maintenance of the earth's electric charge  
The Observatory, 45, 393.
- WILSON, C. T. R. (1929) J. Franklin Inst., 209, 1-12.
- WORKMAN, E. J.,  
HOLZER, R. E. and  
PELSOR, G. T. (1942) The electrical structure of thunderstorms  
N.A.C. Tech. Notes, No.864.
- WORMELL, T. W. (1939) The effects of thunderstorms and lightning discharges on the earth's electric field  
Phil. Trans. A, 238, 249-303.